2024, 21(5): 1512-1535
https://dx.doi.org/10.21123/bsj.2023.8365
P-ISSN: 2078-8665 - E-ISSN: 2411-7986
Baghdad Science Journal

Synthesis, Characterization, Thermal Studies and Antioxidant Activities of Transition Metal Complexes with Azo Dye ligand

Amnah Mahdi Abdullah , ***Abbas Ali Salih Al-Hamdani****

Department of Chemistry, College of Science for Women, University of Baghdad, Baghdad, Iraq.
*Corresponding Author.

Received 14/01/2023, Revised 31/03/2023, Accepted 02/04/2023, Published Online First 20/10/2023, Published 01/05/2024

Abstract

Diazotization reaction between 1-(2,4,6-Trihydroxy-phenyl)-ethanone and diazonium salts was carried out resulting in ligand 4-(3-Acetyl-2,4,6-trihydroxy-phenylazo)-N-(5-methyl-isoxazol-3-yl)-benzenesulfonamide, this in turn reacted with the next metal ions (V^{4+} , Cr^{3+} , Mn^{2+} and Cu^{2+}) forming stable complexes with unique geometries such as (Octahedral for both Cr^{3+} , Mn^{2+} and Cu^{2+} ,squar pyramidal for V^{4+}). The creation of such complexes was detected by employing spectroscopic means involving ultraviolet-visible which proved the obtained geometries, fourier transfer proved the formation of azo group and and the coordination with metal ion through it. Pyrolysis (TGA & DSC) studies proved the coordination of water residues with metal ions inside the coordination sphere as well as chlorine atoms. Moreover, element micro-analysis and AAS that gave corresponding outcome with theoretically counting outcome. (^{1}H &^{13}C-NMR) and magnetic quantifications can also indicate the formation of ligand-H_3L and occurrence of coordination. The thermodynamic constants (ΔH, ΔS and ΔG) were calculated. The DPPH radical scavenging method will be used to assess the antioxidant activities of the compounds the compounds showed antioxidant abilities to scavenge free radical.

Keywords: Antioxidant, Azo dye, Mass spectroscopy, 1-(2,4,6-Trihydroxy-phenyl)-ethanone , Thermal analysis.

Introduction

Diverse types of dyes, often containing highly toxic metal complexes, have been used for the textile industry, and other uses in industries like food industry, leather processing, papermaking, printing, paints, as well cosmetics also it constitutes a source of grave concern to the environment through to its discharge into fresh waters [1]. Their relative importance continues to increase in the future and drive the color and print market decisively[2]. Because azo group has several advantages, it has been used in photochromic, oxidation- responsive, pH sensitive, it stabilizes oxidation state of low-valent metals due to the existence for the a low-lying azo fastened π* molecular orbital, it is utilized as a metal ion indicator at complex measurement titration, dyes as well pigments at textile industry [3] .These azo dye molecules make up over 70% of the entire amount of dye used and have been reported to be mutagenic, carcinogenic, and genotoxic to humans and other aquatic life[4-6].Numerous uses of the dye's related

2024, 21(5): 1512-1535
https://dx.doi.org/10.21123/bsj.2023.8365
P-ISSN: 2078-8665 - E-ISSN: 2411-7986
Baghdad Science Journal

electrolytes, from biology to the textile industry, have been discovered. If the dye is cytotoxic, it can be administered to the living cells after being wrapped in many electrolytes to boost its biocompatibility. Additionally, pH detection is done using the dyes entrapped within the polyelectrolyte complexes [7]. The textile business has been revolutionized by polymer coloring reactions[8,9]. In the production of food, essential electrolytes and edible dyes are frequently used[10]. Biological research have also discovered extensive usage for the combination of colors and proteins[11,12]. Azo dyes of sulfonamides are well known for their antiseptic activity and some of them are useful as chemotherapeutic agents[13]. Transition metals such as V^{4+}, Cr^{3+}, Mn^{2+} and Cu^{2+} have been used in medicine for a long time[14]. Many metal sulfonamide complexes have been shown to be more potent than the parent sulfonamides[15].Because of their interesting bioactivity, many studies have been performed on heterocyclic azo dyes and their metal chelate [16,17]. Azo dye metal chelates are of interest for use in molecular memory storage, non-linear visual representations, and printing systems. The aim of this work is to synthesize a novelmetal ions complexes V^{4+} , Cr^{3+} , Mn^{2+} and Cu^{2+} from azo ligand H_3L as well as characterization with spectroscopic analysis and studying of thermal decomposition and thermal stability by using DSC and TGA curve, the DSC curve was used to calculated thermodynamic parameters ΔH, ΔS and ΔG then antioxidant activity of these compounds was determined against the DPPH radical and compared to that of a standard natural antioxidant gallic acid.

Materials and Methods

Materials have been obtained from the trading suppliers, (SigmaAldrich, Merck, and others). The Urovector model EA/3000, singleV3O, has been employed to achieve (C.H.N. Sand O). Mineral-ions have determined as M-O employing a gravimitrec-approaches. Molar-conductivity has been estimated employing conduct meter W-T-W, 25°C . 1×10^{-3} M. DMSO has been employed as solvent. Mass-spectra for substances have been collected using mass spectrometry (MS) Q-P-50-A-D-I Analysis Shimadzu QP(E170Ev) -2010-Pluss spectrometer. The UV-visible absorption spectra were obtained using a UV-1800 Shimadzu Spectrophotometer. The Brucker (400MHz) Spectrometer was used to obtain the ^{1}H & ^{13}C NMR spectra. The IR Prestige-21 was used to investigate the Fourier Transform Infrared (FTIR) spectra, where the device used was Shimadzu 4000-200 cm^{-1} by CsI and Braker 4000-500 cm^{-1} by KBr. Utilizing a Shimadzu (A.A) 680 G atomic clock, metals were identified. The balancing susceptibility model MSR-MKI was utilized magnetic characteristics. Perkin-Elmer Pyris Diamond DSC/TGA was used for all prior sorts thermal analysis.

Synthesis of Azo Dye Ligand [4-(3-Acetyl-2,4,6-trihydroxy-phenylazo) -N- (5- methyl – isoxazol -3- yl) – benzene sulfon amide] :

Sulfamethoxazole (1g, 3.948mmol) has been dissolved in (2ml HCl , 10ml of ethanol) at 0-5°C during refrigeration. To minimize temperature to 5°C, (10% , 1g , 14.49mmol) $NaNO_2$ were added gradually. After the reaction has been stirred for approximately 45 minutes, (0.663g, 3.948mmol) of 1-(2,4,6-Trihydroxy-phenyl)-ethanone dissolved in 15ml of ethanol were added. A change to a dark colored solution was observed after stirring for 30 minutes to carry out the reaction. This product was collected after being filtered and dried. Its melting point was 146-148 °C and orange precipitate, and its yield was 93%. Scheme1 shows the formation of the ligand azo dye.

General Approach for Metal Complexes Synthesis:

The metal salt (1mmol) [$VOSO_4.5H_2O$ 0.13641g, $CrCl_3.6H_2O$ 0.26649g, $MnCl_2.4H_2O$ 0.19794g and $CuCl_2.2H_2O$ 0.17055g] was dissolved in 10ml of water. (15ml) from Azo ligand H_3L (0.432g, 1mmol) was added drop by drop. The resultant mixture is heated and refluxed for 2 hours up to 40°C . The solid complexes were separated and any unreacted

2024, 21(5): 1512-1535
https://dx.doi.org/10.21123/bsj.2023.8365
P-ISSN: 2078-8665 - E-ISSN: 2411-7986
Baghdad Science Journal

components were removed by briefly immersing them in hot ethanol. The complexes were collected, dried and weighed. Schem1 shows the formation of the metal ions complexes.

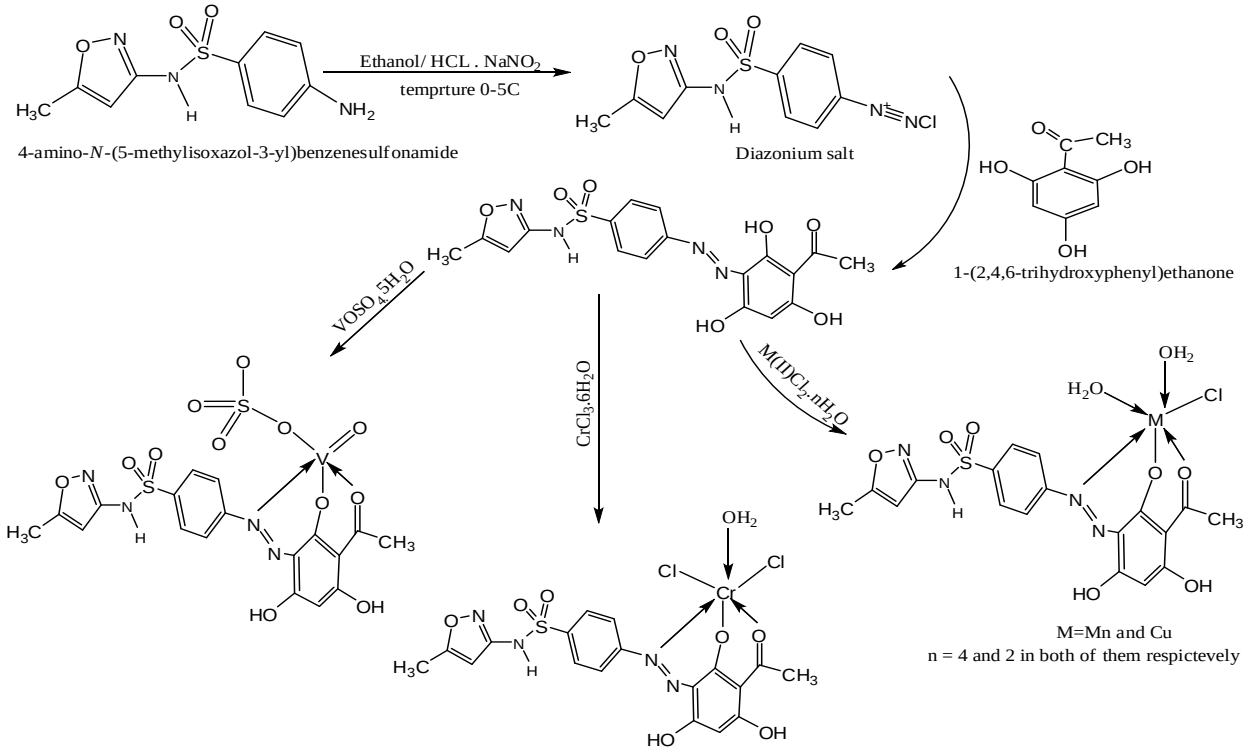

Scheme1. Formation for ligand (H_3L) and their metal complexes

Results and Discussion

Physical and Analytical Data For ligand(H_3L) and the Complexes Synthesized

Reactions of metal salts with ligand gave the synthetic complexes, Scheme 1. The results of elemental analysis demonstrates 1:1 M: L stoichiometry for all complexes .The elemental analysis results were compatible with theoretical calculated results as denoted in Table 1.

Table 1. Some physical properties element micro analysis studies of ligand and complexes.

Compounds formula M.wt	Micro elemental analysis (Found)and Calculated %								
	C	H	N	O	S	M	Cl	Color	m.p °C
H_3L= $C_{18}H_{16}N_4O_7S$ 432=	(50.55) 50.00	(4.01) 3.72	(14.00) 12.96	(25.10) 25.90	(6.70) 7.42	--	--	Orange	**146_148**
$C_{18}H_{15}N_4O_{12}S_2V$ = 593.9415	(36.99) 36.37	(3.59) 2.52	(10.70) 9.43	(31.45) 32.33	(9.88) 10.77	(8.01) 8.58	Nil	Dark Brown	**227_228 d**
$C_{18}H_{17}N_4O_8SCl_2Cr$ 571.99=	(38.07) 37.76	(2.39) 2.97	(10.89) 9.79	(21.86) 22.38	(4.98) 5.60	(10.00) 9.09	(11.80) 12.41	Dark Brown	**300>**
$C_{18}H_{19}N_4O_9SClMn$ 577.44=	(38.02) 38.75	(2.61) 3.40	(11.12) 10.05	(25.00) 25.83	(6.02) 5.74	(10.01) 9.86	(7.22) 6.37	Reddish Brown	**172_174 d**
$C_{18}H_{19}N_4O_9SClCu$ = 566.43	(37.33) 38.16	(3.23) 3.36	(10.10) 9.89	(26.06) 25.44	(5.43) 5.65	(10.93) 11.23	(7.01) 6.27	Brown	**222_223 d**

d=decompose

2024, 21(5): 1512-1535
https://dx.doi.org/10.21123/bsj.2023.8365
P-ISSN: 2078-8665 - E-ISSN: 2411-7986
Baghdad Science Journal

Nuclear Resonance Spectrum of Ligand (^{1}H-NMR &^{13}C-NMR) :

The ^{1}H-NMR &^{13}C-NMR spectrum of newazo, which can be seen in Fig.1 demonstrates the chemical shifts of these spectra. ^{1}H-NMR(DMSO-d_6,ppm):1.92ppm(3H)S, CH_3, 2.08ppm(3H)S, CH_3, 2.38-2.64ppm, DMSO, 3.34ppm(DHO), 6.43ppm, (1H)S,(C-H), 6.77ppm, (1H)S, (C-H) bside OH, 7.26(1H)S,NH, 7.71ppm(1H)d, C-H aromatic bside SO_2 , 7.72ppm, (1H)d (C-H) aromatic bside SO_2 , 8.11ppm, (1H)d (C-H)aromatic bside(N=N), 8.10ppm, (1H)S (C-H)aromatic bside(N=N), 8.74ppm(1H)S, (OH) phenolic bside (N=N), 8.75ppm, (1H)S (OH) phenolic bside(N=N) and 12.00ppm, (1H)S, (OH) phenolic bside $COCH_3$. ^{13}C-NMR: 33.62(C_1), 181.97(C_2), 118.20(C_3) , 165.30(C_4), 157.23(C_5), 155.15(C_6), 145.00(C_7), 172.24(C_8), 137.27(C_9), 148.96(C_{10}), 132.21(C_{11}), 178.10(C_{12}), 106.90(C_{13}), 189.75(C_{14}), 127.48(C_{15}), 169.75(C_{16}), 196.20(C_{17}), and 49.71(C_{18})[18,19].

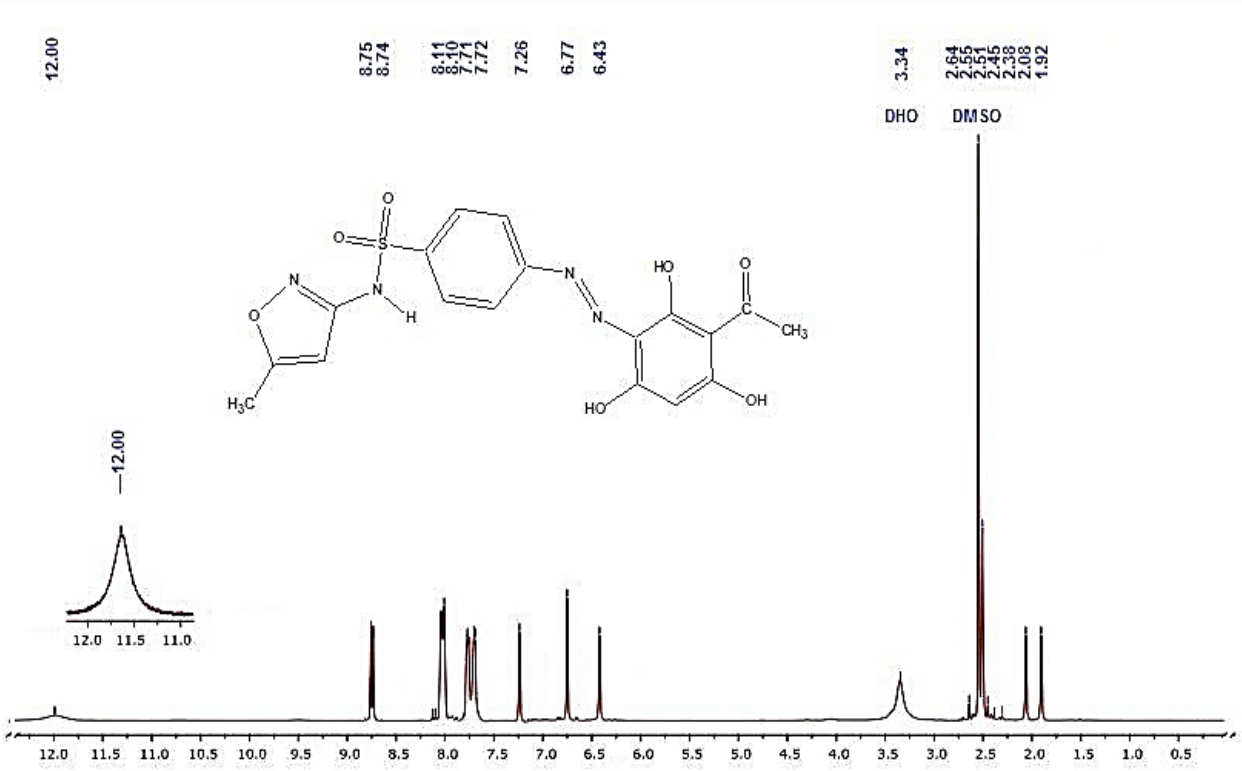

2024, 21(5): 1512-1535
https://dx.doi.org/10.21123/bsj.2023.8365
P-ISSN: 2078-8665 - E-ISSN: 2411-7986
Baghdad Science Journal

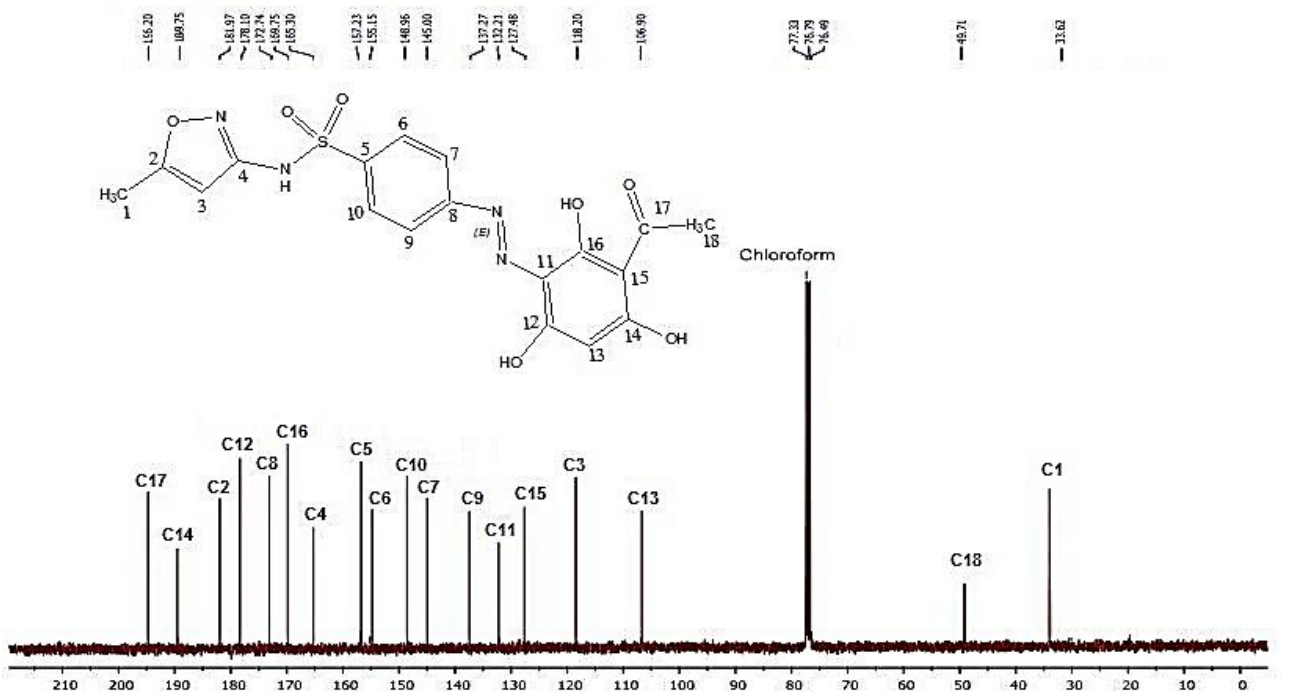

Figure 1. ^{1}H &^{13}C-NMR spectra of ligand (H_3L)

UV-Vis Studies of the Ligand (H_3L) and its Complexes:

The electronic spectrum for ligand (H_3L) in Fig.3 exhibits strong absorpans at 286 nm, 34965.04cm^{-1} ascribed to the π ⟶ π* transition and peak at (392nm, 25510.20cm^{-1}) attributed to the n⟶π* transition a peak with a high intensity band formed withabsorption maxima[20]. The electronic transition of V^{4+}complexe is shown in Fig .2 which depicts a peak of 269, 380, 661 and 850 nm assigned to π→ π*, n→ π*, $^{2}B_2g\rightarrow{}^{2}Eg$ and $^{2}B_2g\rightarrow{}^{2}B_1g$ respectively which is an indicative of a square pyramidal geometry. The Cr^{3+}complex exhibited peaks of 264, 415, 646, 755 and 851 nm ascribed to the π→ π*, n→ π*, and C.T, $^{4}A_2g\rightarrow{}^{4}T_1g_{(P)}$, $^{4}A_2g\rightarrow{}^{4}T_1g_{(F)}$ and $^{4}A_2g\rightarrow{}^{4}T_2g_{(F)}$ respectively. This is in a good agreement with prior work on octahedral geometry[21]. The electronic absorption of Mn^{2+}complexe exhibited peaks of 242, 275, 410, 611, 670, 745 and 787 nm ascribed to the π → π*, n → π*, C.TML,$^{6}A_1g\rightarrow{}^{4}Eg_{(G)}$, $^{6}A_1g\rightarrow{}^{4}T_2g_{(G)}$,$^{6}A_1g\rightarrow{}^{4}T_1g_{(G)}$and $^{6}A_1g\rightarrow{}^{4}T_2g_{(D)}$ respectively which is an indicative of a Octahedral geometry [22]. The Cu^{2+}complexe exhibited peaks at 245, 575, 398 and 795 nm ascribed to the π→ π*,n→ π*, C.TML and $^{2}Eg\rightarrow{}^{2}T_2g$ respectively. which is in a good agreement with prior work on Octahedral geometry [23]. Table 2 displays the electronic assignment, metal complexes.

2024, 21(5): 1512-1535
https://dx.doi.org/10.21123/bsj.2023.8365
P-ISSN: 2078-8665 - E-ISSN: 2411-7986
Baghdad Science Journal

Table 2. UV-Vis spectra, magnetic moments and molar conductivity for ligand (H_3L) and their metal complexes

Compound	λ nm	ύ cm^{-1}	Abs	$Ɛ_{max}$ L mol^{-1} cm^{-1}	Assignment	$μ_{eff}$ (B.M)	Λm $S.cm^2.Mol^{-1}$
Ligand = H_3L	286	34965.04	1.602	16020	π →π*	--	--
	392	25510.20	1.732	17320	n→ π*		
$VO(H_2L)(SO_4)$] [Square pyramidal	269	37174.72	2.998	29980	π→π*	1.63	12
	380	26315.79	1.100	11000	n→π*		
	661	15128.59	0.410	4100	$^2B_2g \rightarrow {}^2Eg$		
	850	11764.71	0.400	4000	$^2B_2g \rightarrow {}^2B_1g$		
]$Cr(H_2L)(H_2O)Cl_2$[Octahedral	264	37878.79	0.512	5120	π→π*	3.81	12
	415	24096.39	0.800	8000	n→π*		
	646	15479.88	0.045	450 250	$^4A_2g \rightarrow {}^4T_1g_{(P)}$		
	755	13245.03	0.025	500	$^4A_2g \rightarrow {}^4T_1g_{(F)}$		
	851	11750.88	0.050		$^4A_2g \rightarrow {}^4T_2g_{(F)}$		
$Mn(H_2L)(H_2O)_2Cl$][Octahedral	242	41322.31	0.500	5000	π→π*	5.70	11
	275	36363.64	0.600	6000	n→π*		
	410	24390.24	1.137	11370	C.T M→L		
	611	16366.61	0.021	210	$^6A_1g \rightarrow {}^4Eg_{(G)}$		
	670	14925.37	0.034	340	$^6A_1g \rightarrow {}^4T_2g_{(G)}$		
	745	13422.82	0.036	360	$^6A_1g \rightarrow {}^4T_1g_{(G)}$		
	787	12706.48	0.024	240	$^6A_1g \rightarrow {}^4T_2g_{(D)}$		
]$Cu(H_2L)(H_2O)_2Cl$[Octahedral	245	40816.32	0.856	856014	π→π*	1.76	20
	275	36363.63	1.457	570	n→π*		
	398	25125.63	0.800	8000	C.T M→L		
	795	12578.62	0.269	2690	$^2Eg \rightarrow {}^2T_2g$		

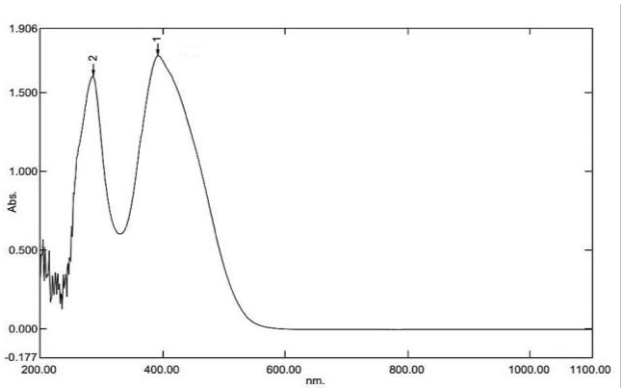

Figure2. UV-Vis spectrum of V-complex

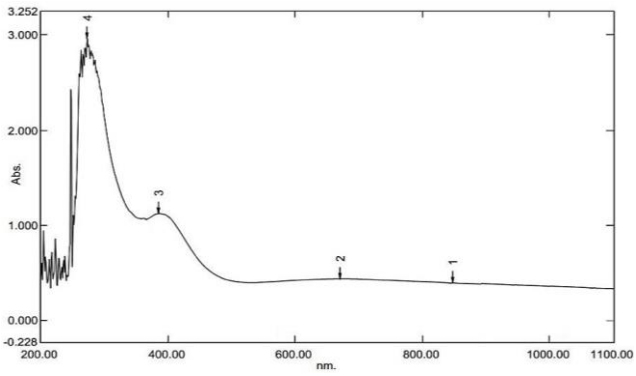

Figure3. UV-Vis spectrum of ligand (H_3L)

LC-Mass Spectrum. of H_3L & Some Products:

LC-Mass spectrumof ligand (H_3L) & some products were tested using LC-Mass device, this approach is one of the most important approaches in characterization and complementary for the rest approaches by which the molecular weight of the compound is estimated according to the relation (m/z). Mass information of the ligand in Scheme 2

2024, 21(5): 1512-1535
https://dx.doi.org/10.21123/bsj.2023.8365
P-ISSN: 2078-8665 - E-ISSN: 2411-7986
Baghdad Science Journal

shows the fragmentation pattern and the extract mass for each pattern. We can clearly observe the molecular ion peak $[M]^+$ for the fragment $C_{14}H_{10}N_2O_6S^{\bullet+}$and its relative abundance about 66% in Fig.4, in addition to other abundances for the rest of peaks including $C_8H_8N_2O_4^{\bullet+}$, $C_6H_4O_2S^{\bullet+}$ and $C_4H_4N_2O^{\bullet+}$ mentioned in Table 3 and corresponded the next abundances: 47%, 33% and79%respectively[24]. For $[VO(H_2L)(SO_4)]$, Fig. 5 and Scheme 3, we can also detect the molecular ion peak (M^+) at 593.96 m/z with relative abundance 20% and next patterns: $C_{18}H_{14}N_4O_8SV^{\bullet+}$, $C_{14}H_9N_2O_5V^{\bullet+}$ and $C_4H_4N_2O_3S^{\bullet+}$, which corresponded to 497 m/z, 335.99 m/z and159.99 m/z respectively[24]. For $[Cr(H_2L)\ (H_2O)\ Cl]$ complex in Fig. 6 and Scheme 4, which illustrate the next fragments: (M^+) at 570.95 m/z with relative abundance 20%, $C_{18}H_{15}Cl_2CrN_4O_7S^+$, $C_{18}H_{15}CrN_4O_7S^{\bullet+}$, $C_5H_6CrO_3^{\bullet+}$, $C_6H_5NO_2S^{\bullet+}$, $C_3H_4N_2O^{\bullet+}$ and $C_4H_4NO^+$ that corresponded to 552.94 m/z, 483.01 m/z, 165.97 m/z, 155 m/z, 84.03 m/z and82.03 m/z respectively [25]. Additionally, $[Mn(H_2L)(H_2O)_2Cl]$ complex in Fig. 7 and Scheme 5, illustrate the next fragments: (M^+) at 556.99 m/z with relative abundance 10%, $C_{18}H_{15}ClMnN_4O_7S^+$, $C_{14}H_{10}ClMnN_2O_4^{\bullet+}$, $C_6H_6ClMnN_2O_2^{\bullet+}$, $C_4H_4N_2O_3S^{\bullet+}$ and $C_8H_7O_2^+$ that correspond to 520.97 m/z, 359.97 m/z, 227.95 m/z, 159.99 m/z and135.04 m/z respectively [25]. Finally, Fig. 8 and Scheme 6 of $[Cu(H_2L)(H_2O)_2Cl]$ complex illustrate the next fragments:(M^+) at 564.99 m/z with relative abundance 10%,$C_{18}H_{15}ClCuN_4O_7S^+$, $C_{14}H_{10}ClCuN_2O4^{\bullet+}$, $C_6H_4ClCuN^{\bullet+}$, $C_8H_7NO4^{\bullet+}$and $C_4H_4N_2O_3S^{\bullet+}$ corresponded to 528.96 m/z, 367.96 m/z , 187.93 m/z, 181.04 m/z and159.99 m/z respectively [25].

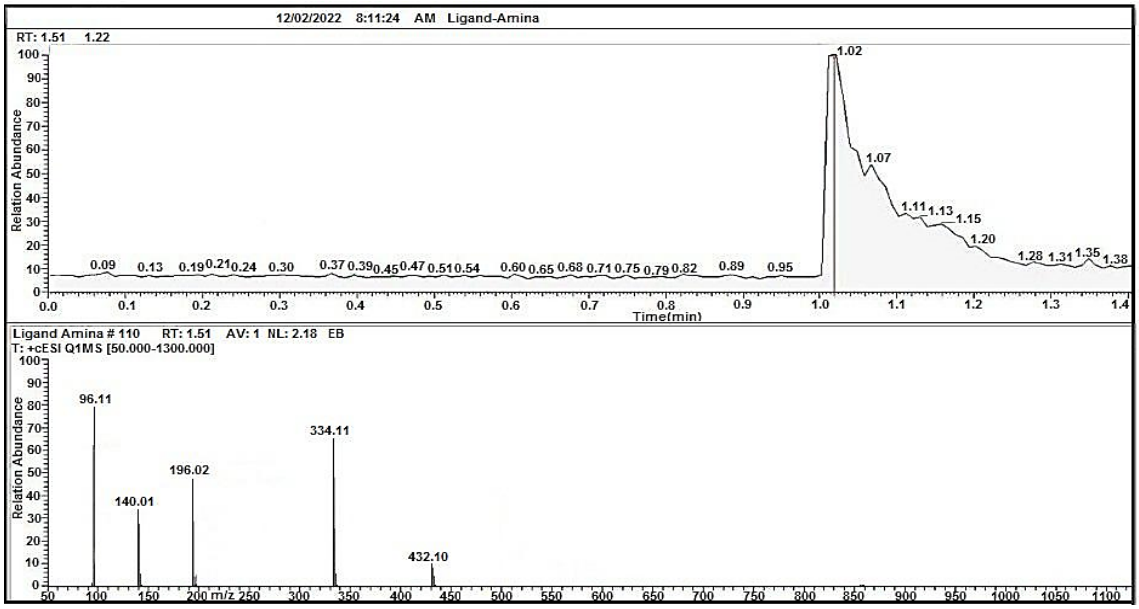

Figure 4. Mass spectrum of ligand

2024, 21(5): 1512-1535
https://dx.doi.org/10.21123/bsj.2023.8365
P-ISSN: 2078-8665 - E-ISSN: 2411-7986
Baghdad Science Journal

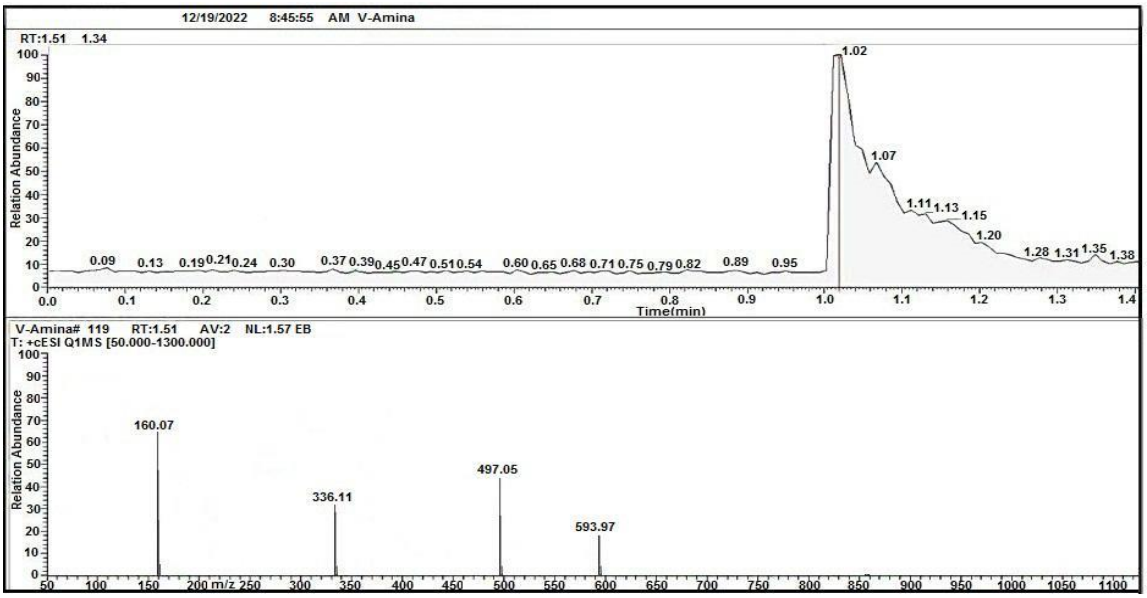

Figure 5. Mass spectrum of V-complex

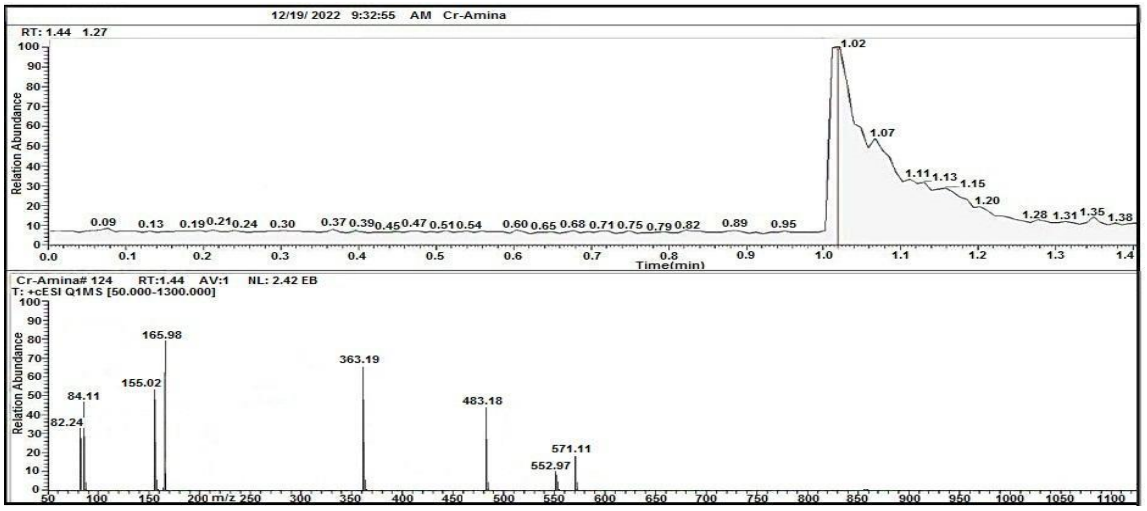

Figure 6. Mass spectrum of Cr-complex

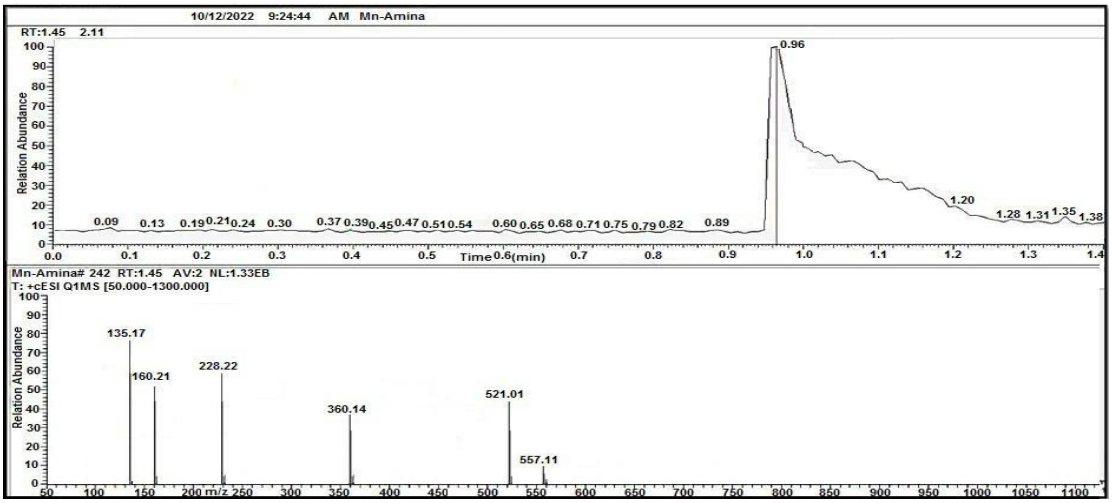

Figure7. Mass spectrum of Mn-complex

2024, 21(5): 1512-1535
https://dx.doi.org/10.21123/bsj.2023.8365
P-ISSN: 2078-8665 - E-ISSN: 2411-7986
Baghdad Science Journal

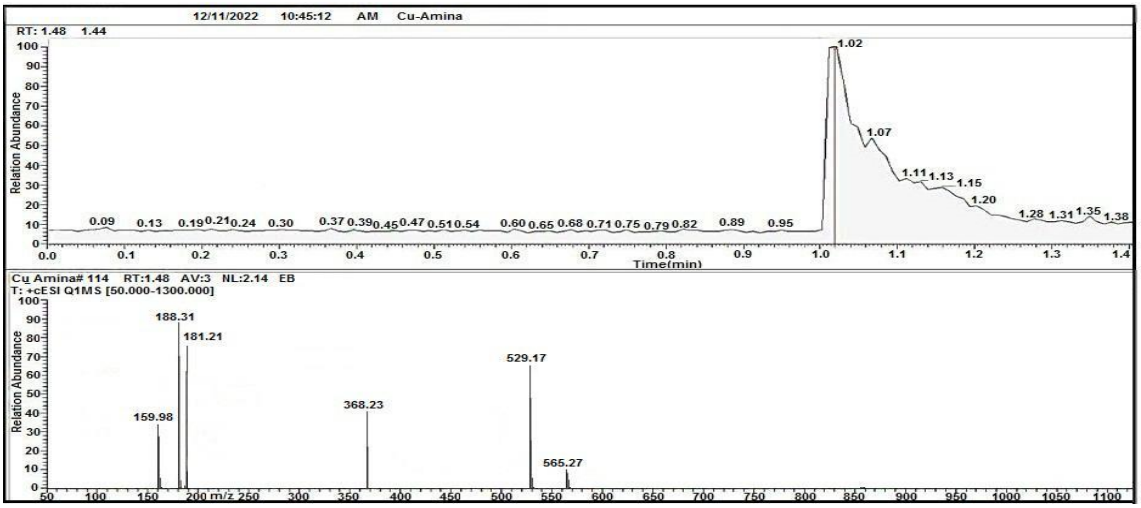

Figure8. Mass spectrum of Cu-complex

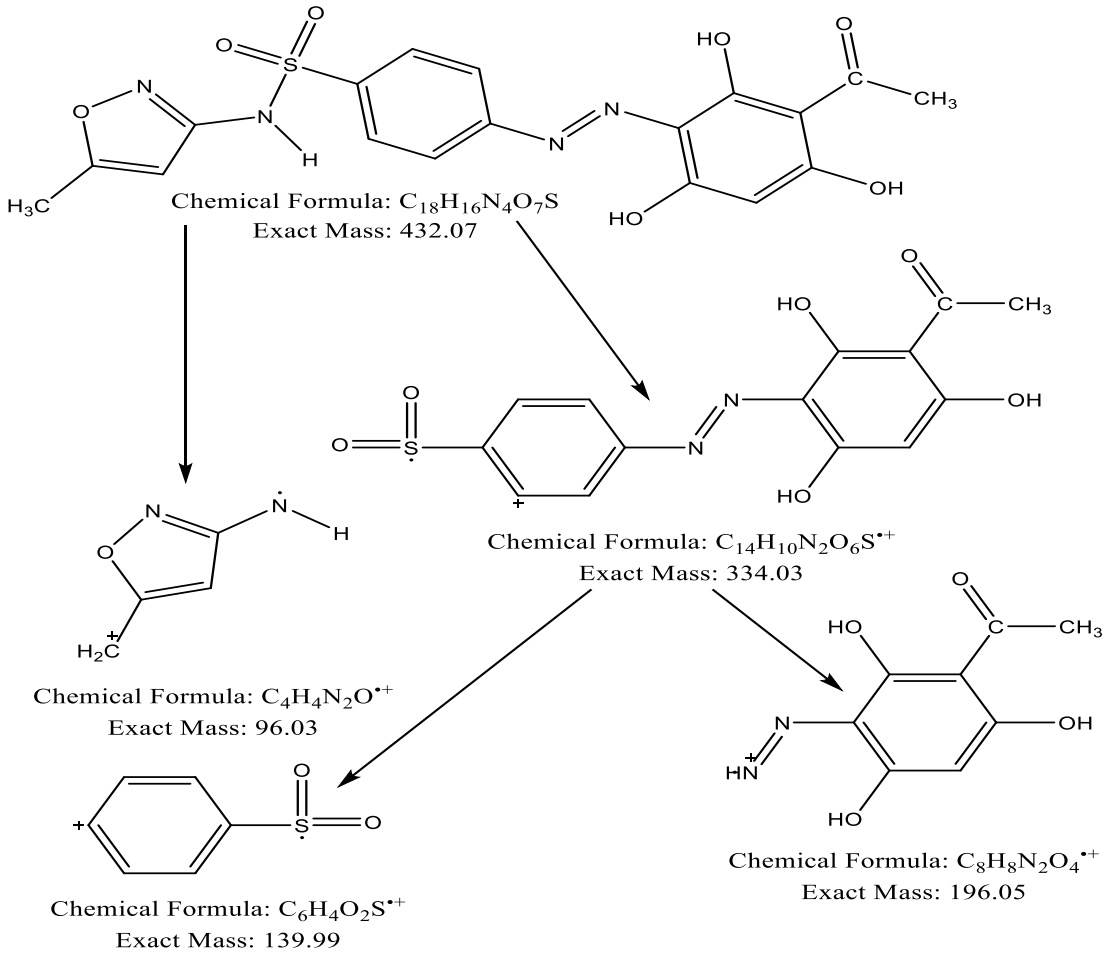

Scheme 2. Pattern of fragmentation of ligand (H_3L)

2024, 21(5): 1512-1535
https://dx.doi.org/10.21123/bsj.2023.8365
P-ISSN: 2078-8665 - E-ISSN: 2411-7986
Baghdad Science Journal

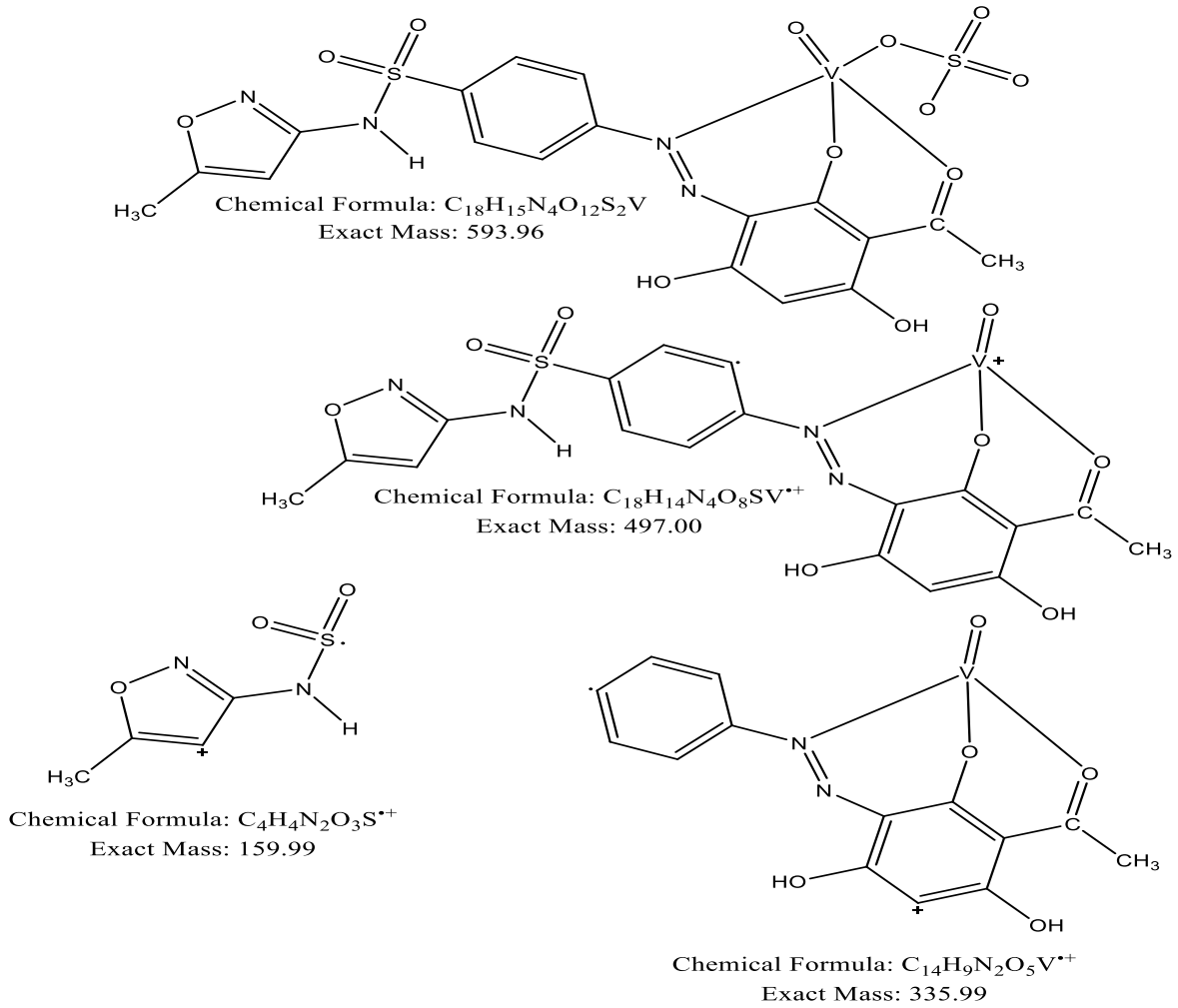

Scheme 3. Pattern of fragmentation of V-complex

2024, 21(5): 1512-1535
https://dx.doi.org/10.21123/bsj.2023.8365
P-ISSN: 2078-8665 - E-ISSN: 2411-7986
Baghdad Science Journal

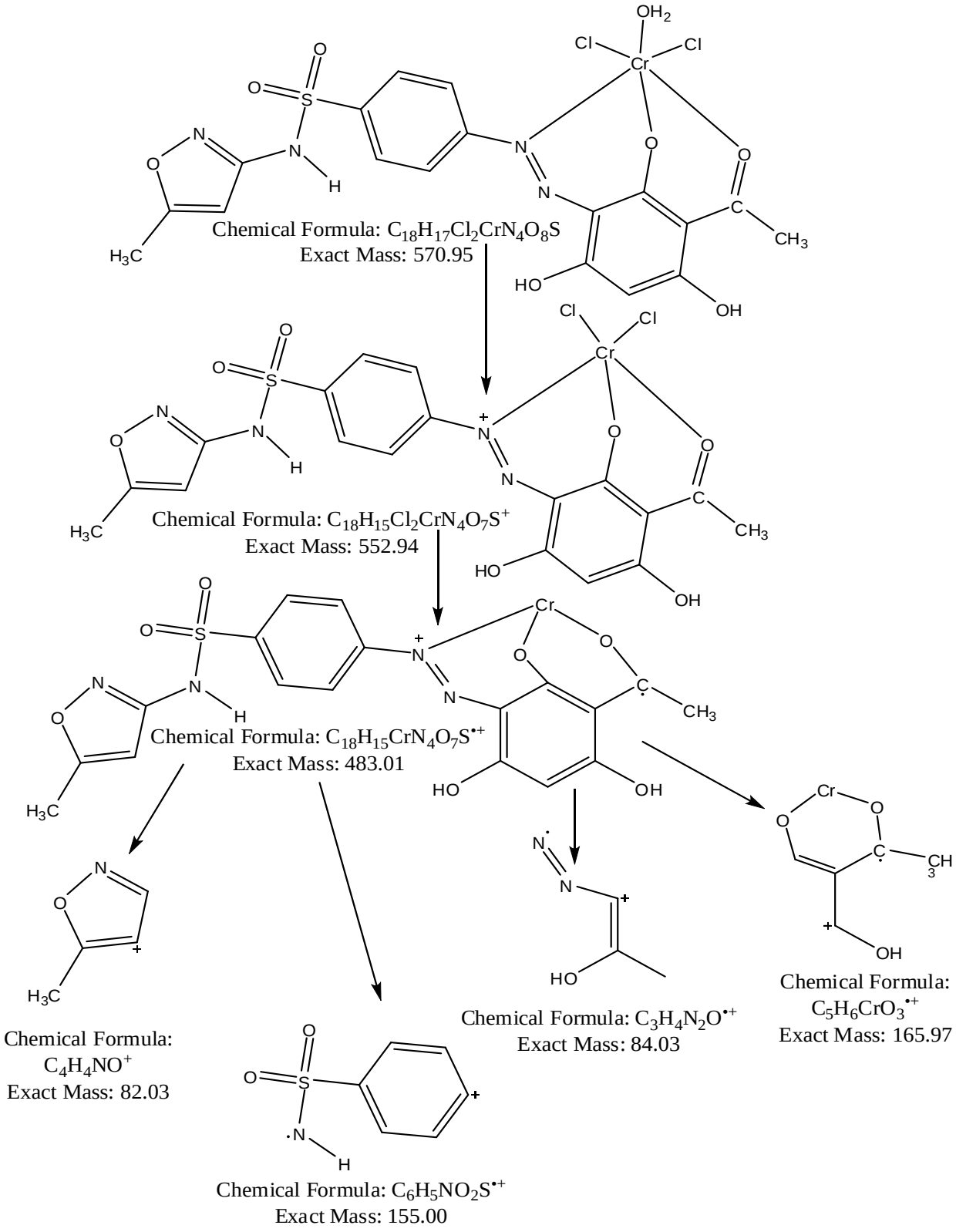

Scheme 4. Pattern of fragmentation of Cr-complex

2024, 21(5): 1512-1535
https://dx.doi.org/10.21123/bsj.2023.8365
P-ISSN: 2078-8665 - E-ISSN: 2411-7986
Baghdad Science Journal

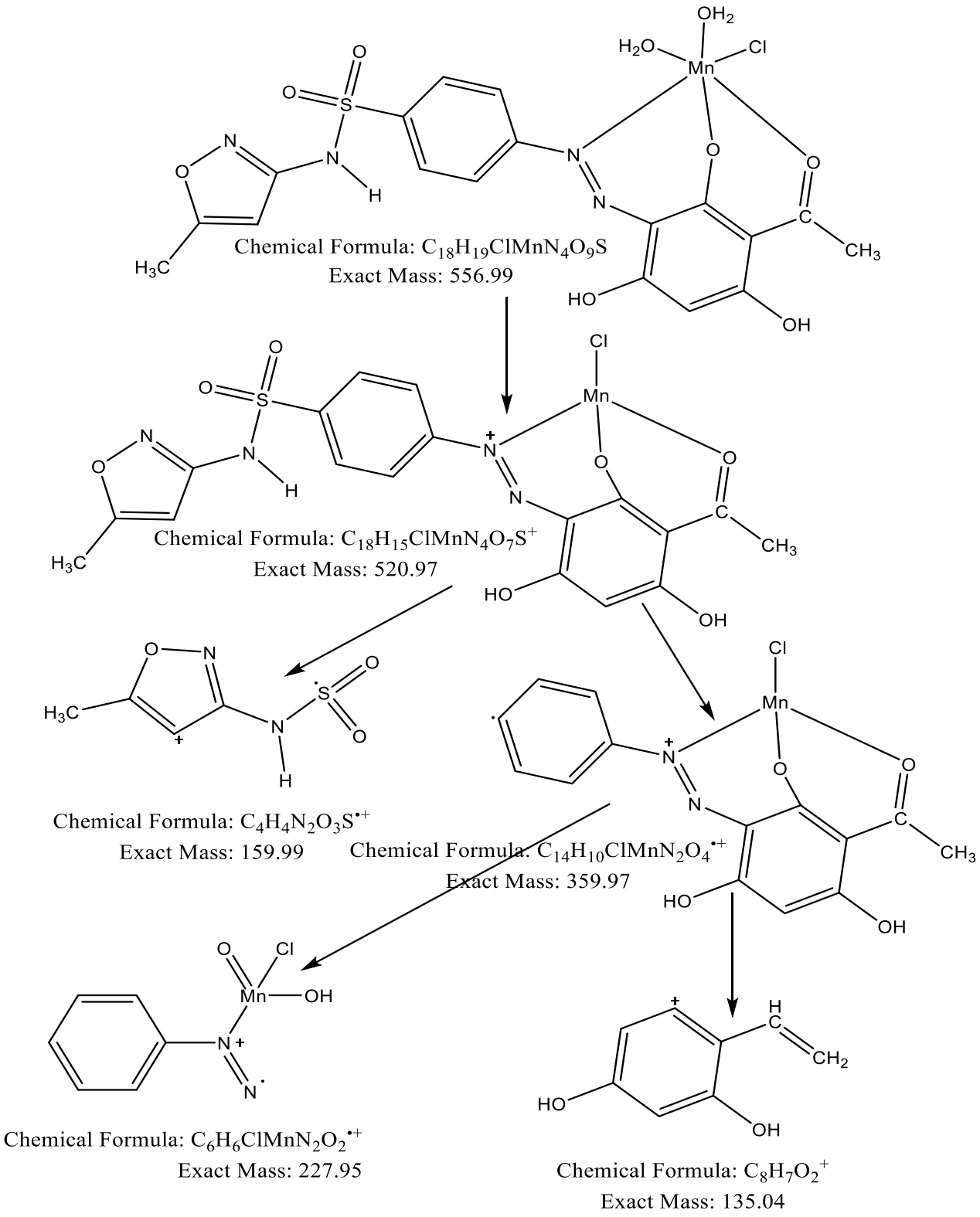

Scheme 5. Pattern of fragmentation of Mn-complex

2024, 21(5): 1512-1535
https://dx.doi.org/10.21123/bsj.2023.8365
P-ISSN: 2078-8665 - E-ISSN: 2411-7986
Baghdad Science Journal

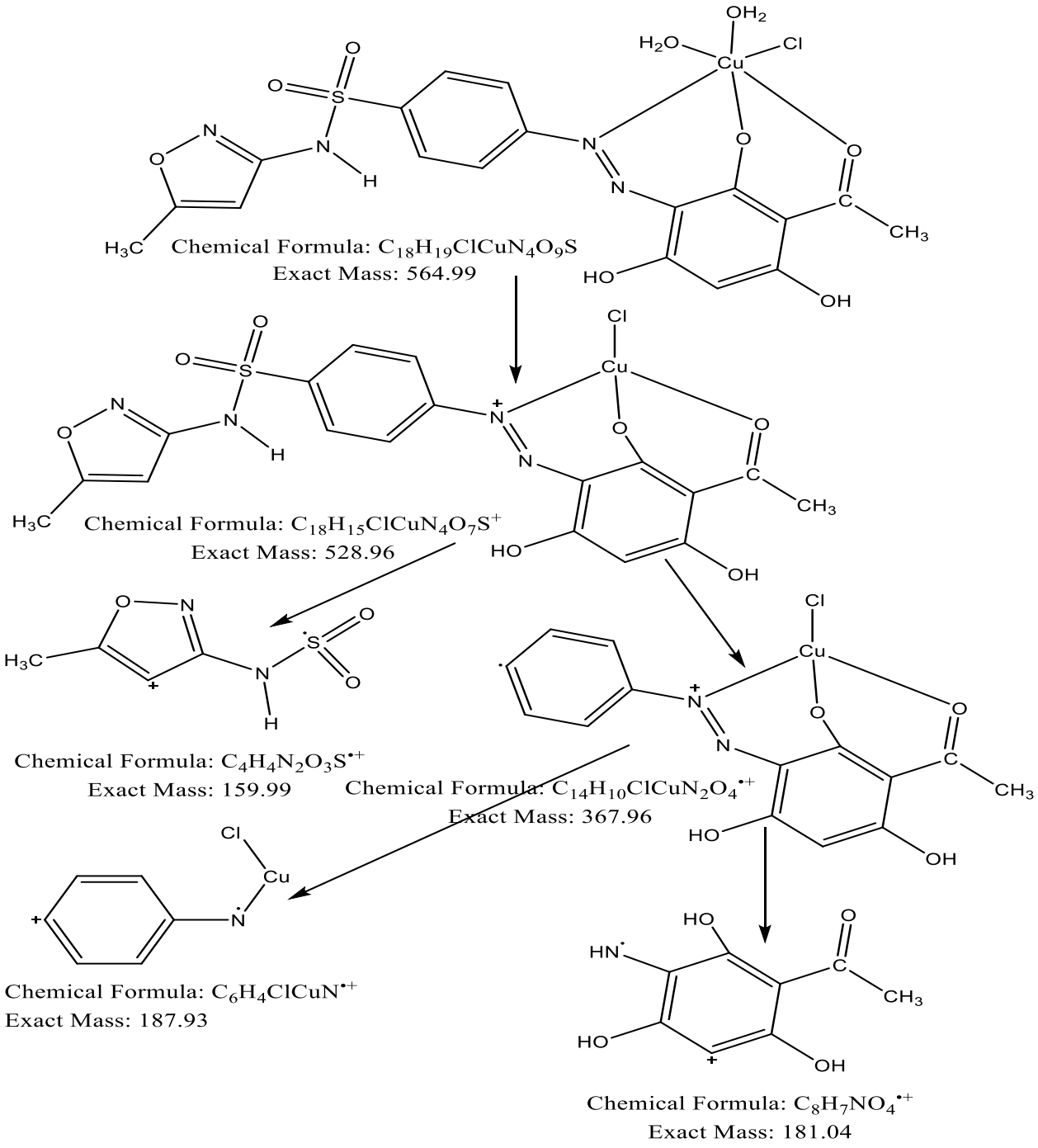

Scheme 6. Pattern of fragmentation of Cu-complex

2024, 21(5): 1512-1535
https://dx.doi.org/10.21123/bsj.2023.8365
P-ISSN: 2078-8665 - E-ISSN: 2411-7986
Baghdad Science Journal

Table 3. LC-Mass spectral data of ligand and its complexes

Fragment	m/z Exact mass	Relative Abundance(%)
]$C_{18}H_{16}N_4O_7S$[	432.07	10
[$C_{14}H_{10}N_2O_6S$]$^{\bullet+}$	334.03	66
[$C_8H_8N_2O_4$]$^{\bullet+}$	196.05	47
[$C_6H_4O_2S$]$^{\bullet+}$	139.99	33
[$C_4H_4N_2O$]$^{\bullet+}$	96.03	79
]$C_{18}H_{15}N_4O_{12}S_2V$[	593.96	18
[$C_{18}H_{14}N_4O_8SV$]$^{\bullet+}$	497.00	44
[$C_{14}H_9N_2O_5V$]$^{\bullet+}$	335.99	33
[$C_4H_4N_2O_3S$]$^{\bullet+}$	159.99	64
[$C_{18}H_{17}Cl_2CrN_4O_8S$]	571.11	19
[$C_{18}H_{15}Cl_2CrN_4O_7S$]$^+$	552.94	10
[$C_{18}H_{15}CrN_4O_7S$]$^{\bullet+}$	483.01	45
[$C_5H_6CrO_3$]$^{\bullet+}$	165.97	80
[$C_6H_5NO_2S$]$^{\bullet+}$	155.00	54
[$C_3H_4N_2O$]$^{\bullet+}$	84.03	47
[C_4H_4NO]$^+$	82.03	32
]$C_{18}H_{19}N_4O_9SClMn$[	556.99	10
[$C_{18}H_{15}N_4O_7SClMn$]$^+$	520.97	45
[$C_{14}H_{10}N_2O_4ClMn$]$^{\bullet+}$	359.97	36
[$C_6H_6N_2O_2ClMn$]$^{\bullet+}$	227.95	59
[$C_4H_4N_2O_3S$]$^{\bullet+}$	159.99	51
[$C_8H_7O_2$]$^+$	135.04	77
]$C_{18}H_{19}N_4O_9SClCu$[	564.99	10
[$C_{18}H_{15}N_4O_7SClCu$]$^+$	528.96	64
[$C_{14}H_{10}N_2O_4ClCu$]$^{\bullet+}$	367.96	41
[C_6H_4NClCu]$^{\bullet+}$	187.93	75
[$C_8H_7NO_4$]$^{\bullet+}$	181.04	89
[$C_4H_4N_2O_3S$]$^{\bullet+}$	159.99	34

Infrared Spectra Measurements:

The azo ligand spectra and their metal chelates complexes with V^{4+}, Cr^{3+}, Mn^{2+} and Cu^{2+} have been compiled, and the data has been organized in Table 4, Fig.9 for the ligand and Fig.10 for the vanadium complex. The ligand displayed bands at 3503, 3281,3014, 2979, 1635 and 1088-1015 cm^{-1} that were ascribed to the ν (OH) phenolic, ν (NH), ν (C-H) aromatic, ν (C-H)aliphatic, ν(C =O) and ν(SO_2).FT-IR spectrum of the resulting ligand demonstrates new distinguishable double band at 1485 cm^{-1} attributed to stretching vibrational behavior of azo group N=N, which indicates the ligand formation. After this, the IR spectra of all produced compounds revealed that the azo-dye ligand connected to metal ions through two sites: the azo group's nitrogen site, and oxygen site via deprotonation of the phenolic [26]. New bands belonging to (M-N) appeared at 549, 520, 501 and 512 cm^{-1} for the V^{4+}, Cr^{3+},Mn^{2+} and Cu^{2+} complexes, respectively, (M-O) at 406, 480, 460 and 450 cm^{-1} for the complexes of V^{4+}, Cr^{3+},Mn^{2+} and Cu^{2+}, respectively, (M-Cl) at 385, 389 and 370 cm^{-1} for the complexes of Cr^{3+},Mn^{2+} and Cu^{2+}, respectively.

2024, 21(5): 1512-1535
https://dx.doi.org/10.21123/bsj.2023.8365
P-ISSN: 2078-8665 - E-ISSN: 2411-7986
Baghdad Science Journal

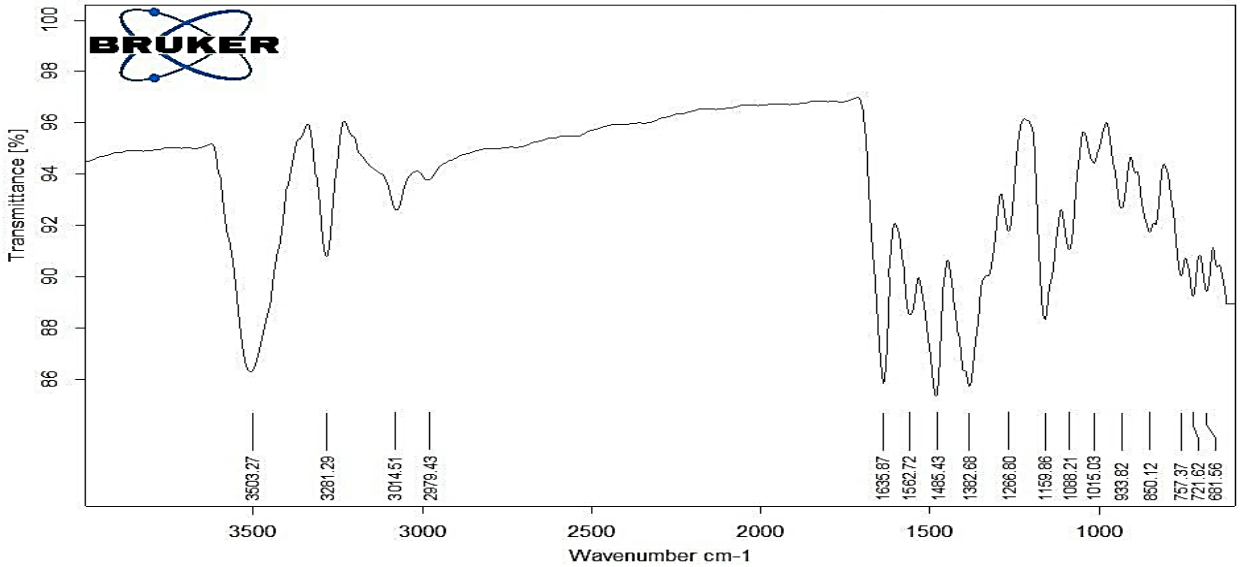

Figure 9. FT-IR spectrum of ligand (H_3L)

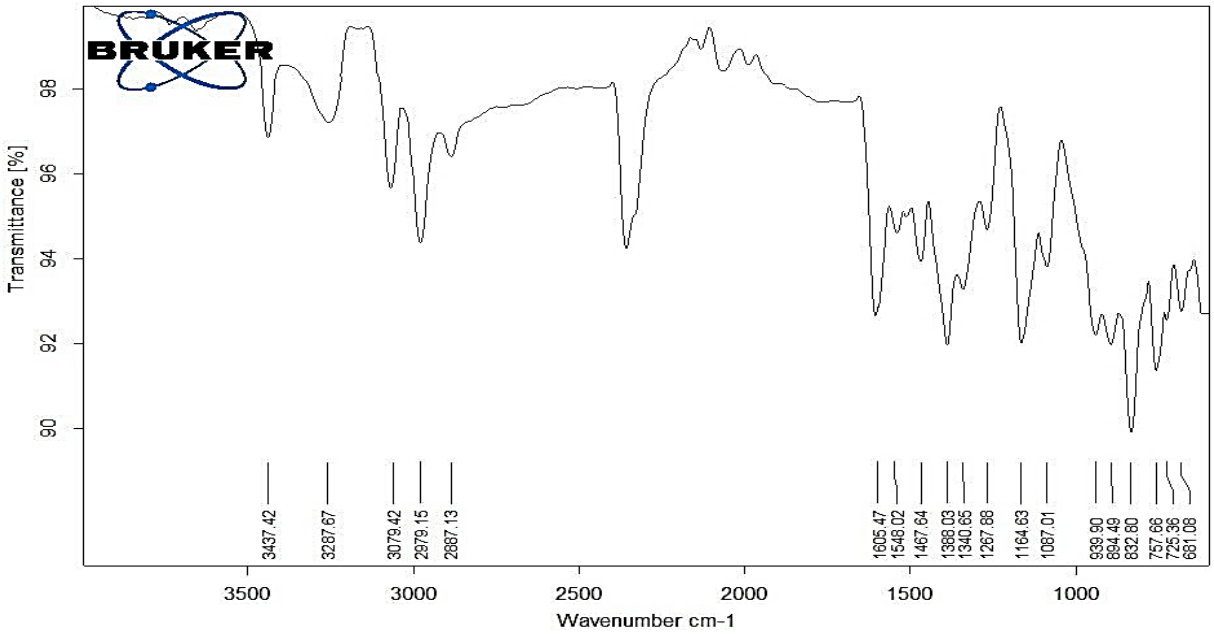

Figure 10. FT-IR spectrum of V-complex

2024, 21(5): 1512-1535
https://dx.doi.org/10.21123/bsj.2023.8365
P-ISSN: 2078-8665 - E-ISSN: 2411-7986
Baghdad Science Journal

Table 4. The IR spectra bands (cm^{-1}) of the ligand azo and its complexes

Compounds	ν (H_2O) aqua	ν (OH) phenolic	ν (NH)	ν (C-H) aromatic aliphatic	ν(C =O)	ν (N=N)	ν(SO_2)	Other bands
H_3L	--	3503	3281	3014 2979	1635	1485	1088 1015	_
$[VO(H_2L)(SO_4)]$	--	3437	3287	3079 2979	1605	1467	1087	549 (V-N) 406 (V-O) 979(V=O
$[Cr(H_2L)(H_2O)Cl_2]$	3739	3501	3285	3067 2927	1605	1467	1089 1005	520 (Cr-N) 480 (Cr-O) 385 (Cr-Cl)
$[Mn(H_2L)(H_2O)_2Cl]$	3738	3504	3283	3049 2977	1603	1467	1010	501 (Mn-N) 460 (Mn-O) 389 (Mn-Cl)
$[Cu(H_2L)(H_2O)_2Cl]$	3704	3520	3284	3070 2983	1603	1473	1087	512 (Cu-N) 450 (Cu-O) 370 (Cu-Cl)

Thermal Study Data:

The findings of the thermal analysis for ligand (H_3L) and their synthesized complexes are displayed in Tables 5, 6, the Figs.11- 14 respectively. Tentative decomposition reaction of metal complexes is summarized in Schemes 5. Decomposition stages, temperature ranges, decomposition products, and weight loss complex percentages were computed based on the thermograms, and they showed agreement between their thermal decomposition results and calculated values, that validates elemental analysis results and suggested Eqs[27,28]. In this work, it was noted that the remaining ligand was carbon and the remaining metal oxide in the ligand and metal complexes of V^{4+}, Cr^{3+} and Mn^{2+}. According to the results of the thermo gravimetric tests, the complexes and the ligand decompose in (one to three) phases. The thermodynamic parameters ΔH, ΔS and ΔG were computed using the DCS curve, as shown in Scheme 7.

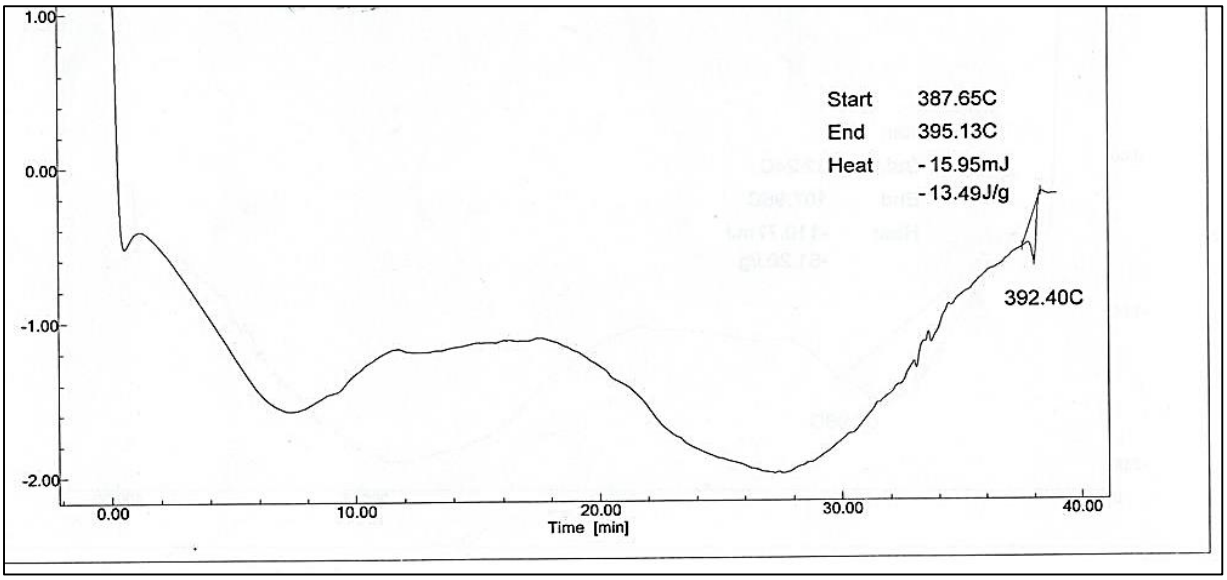

Figure 11. TGA&DSC curve of Ligand (H_3L)

2024, 21(5): 1512-1535
https://dx.doi.org/10.21123/bsj.2023.8365
P-ISSN: 2078-8665 - E-ISSN: 2411-7986
Baghdad Science Journal

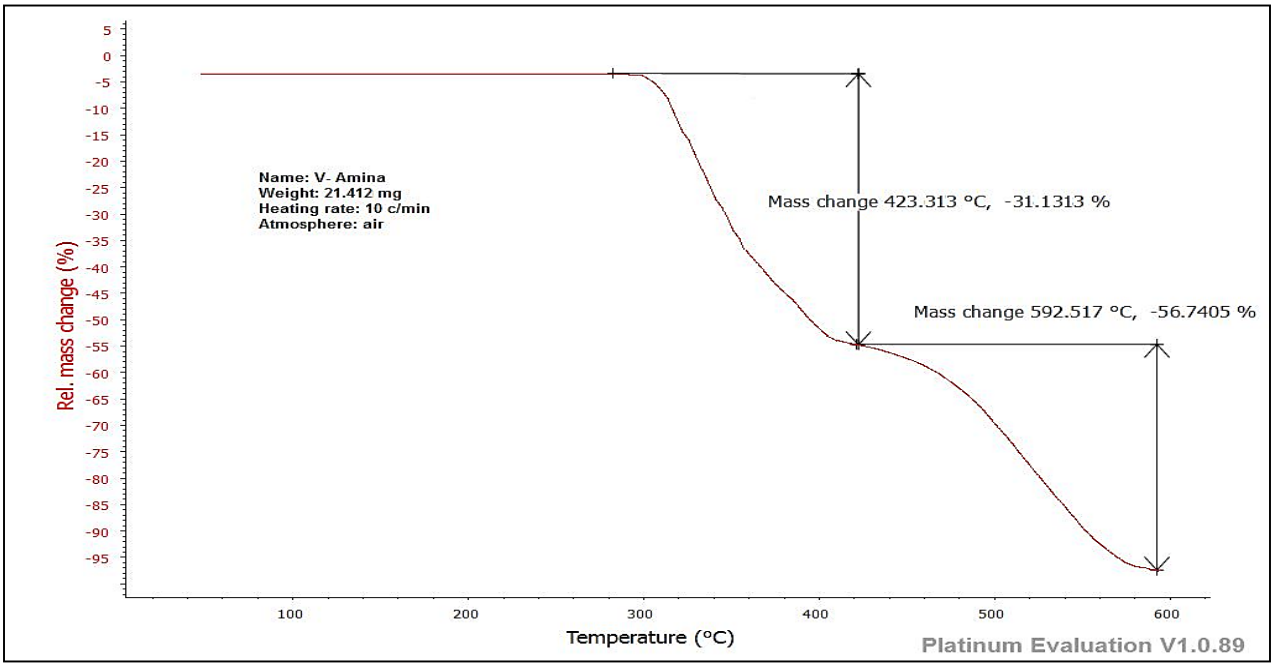

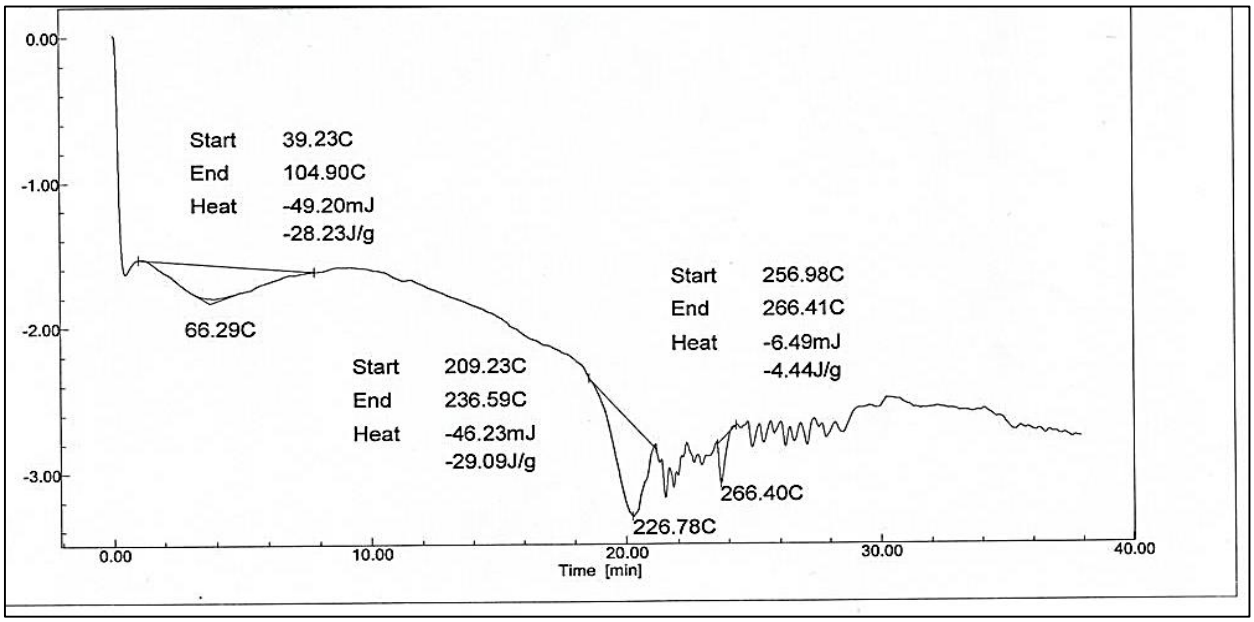

Figure 12. TGA & DSC curve of V-complex

2024, 21(5): 1512-1535
https://dx.doi.org/10.21123/bsj.2023.8365
P-ISSN: 2078-8665 - E-ISSN: 2411-7986
Baghdad Science Journal

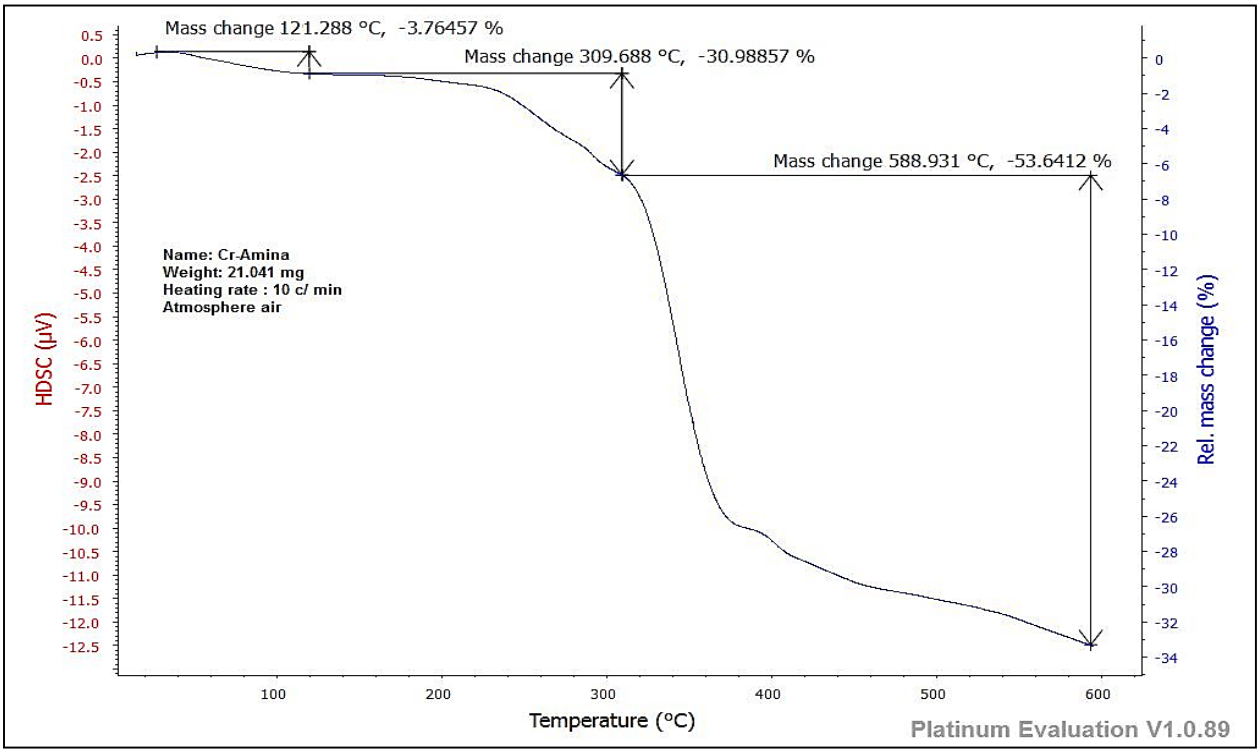

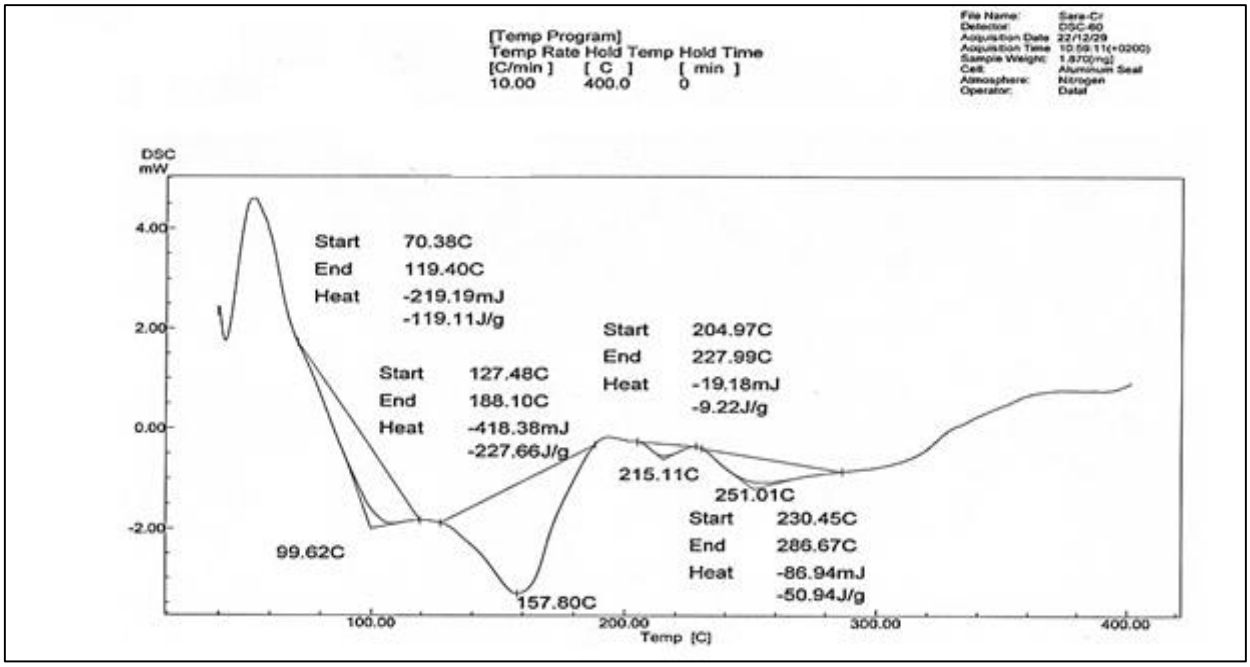

Figure 13. TGA & DSC curve of Cr-complex

2024, 21(5): 1512-1535
https://dx.doi.org/10.21123/bsj.2023.8365
P-ISSN: 2078-8665 - E-ISSN: 2411-7986
Baghdad Science Journal

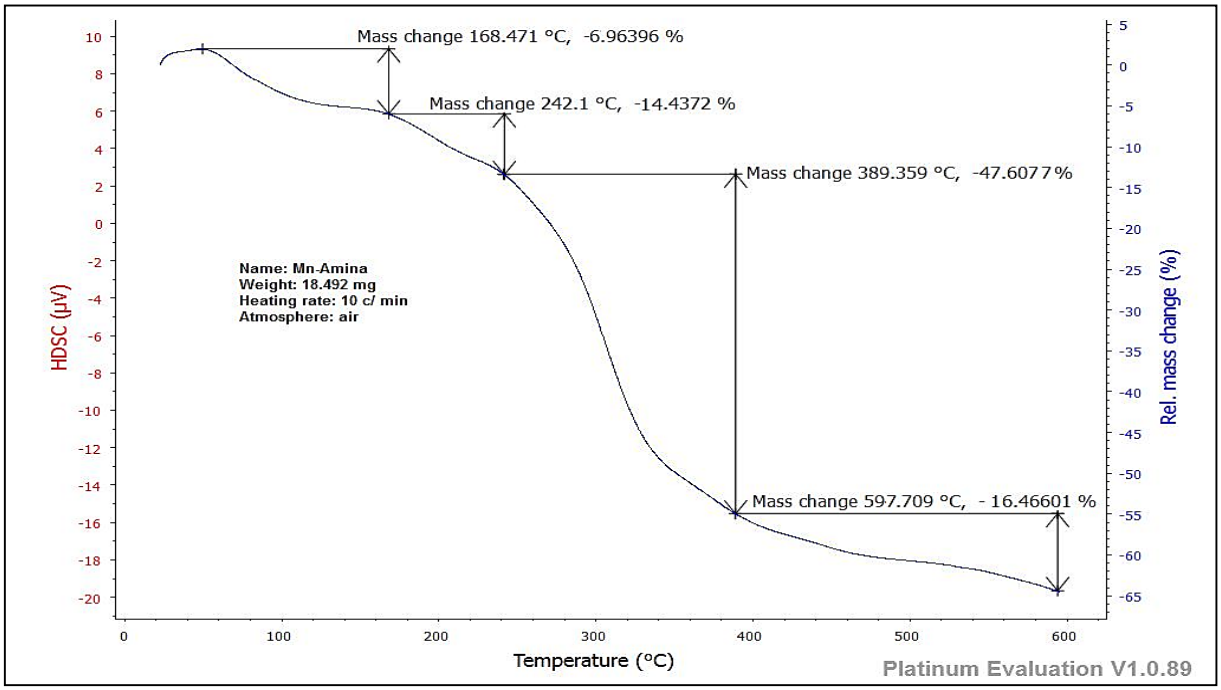

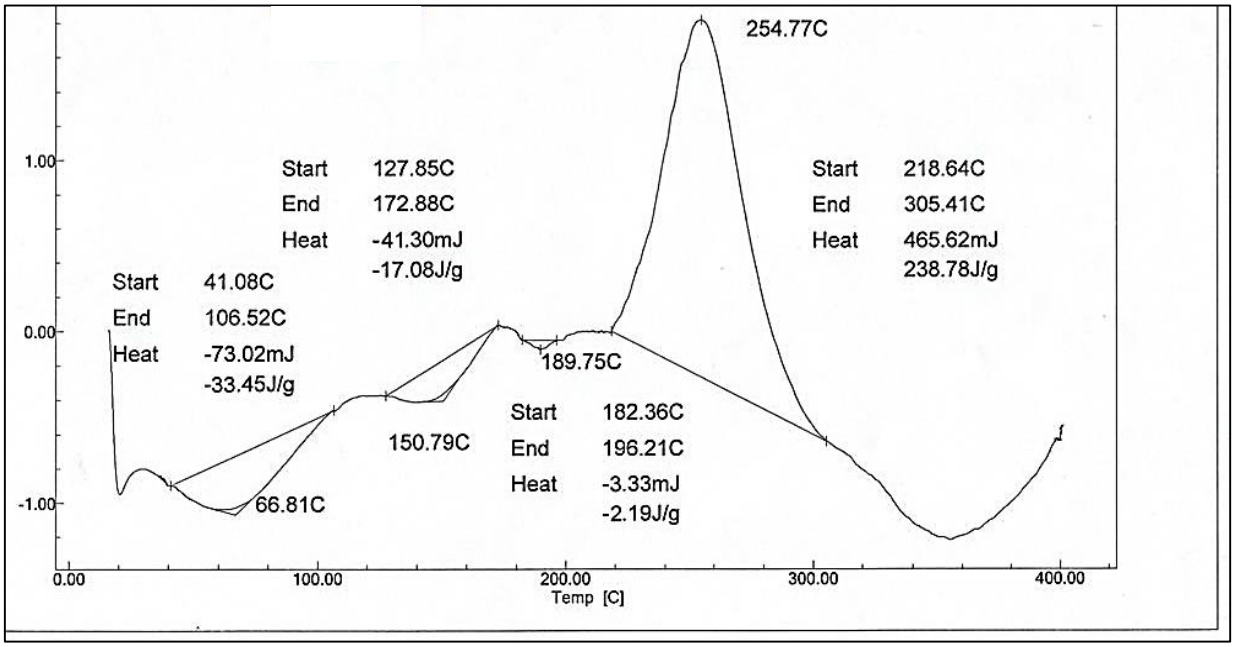

Figure 14. TGA & DSC curve of Mn-complex

2024, 21(5): 1512-1535
https://dx.doi.org/10.21123/bsj.2023.8365
P-ISSN: 2078-8665 - E-ISSN: 2411-7986
Baghdad Science Journal

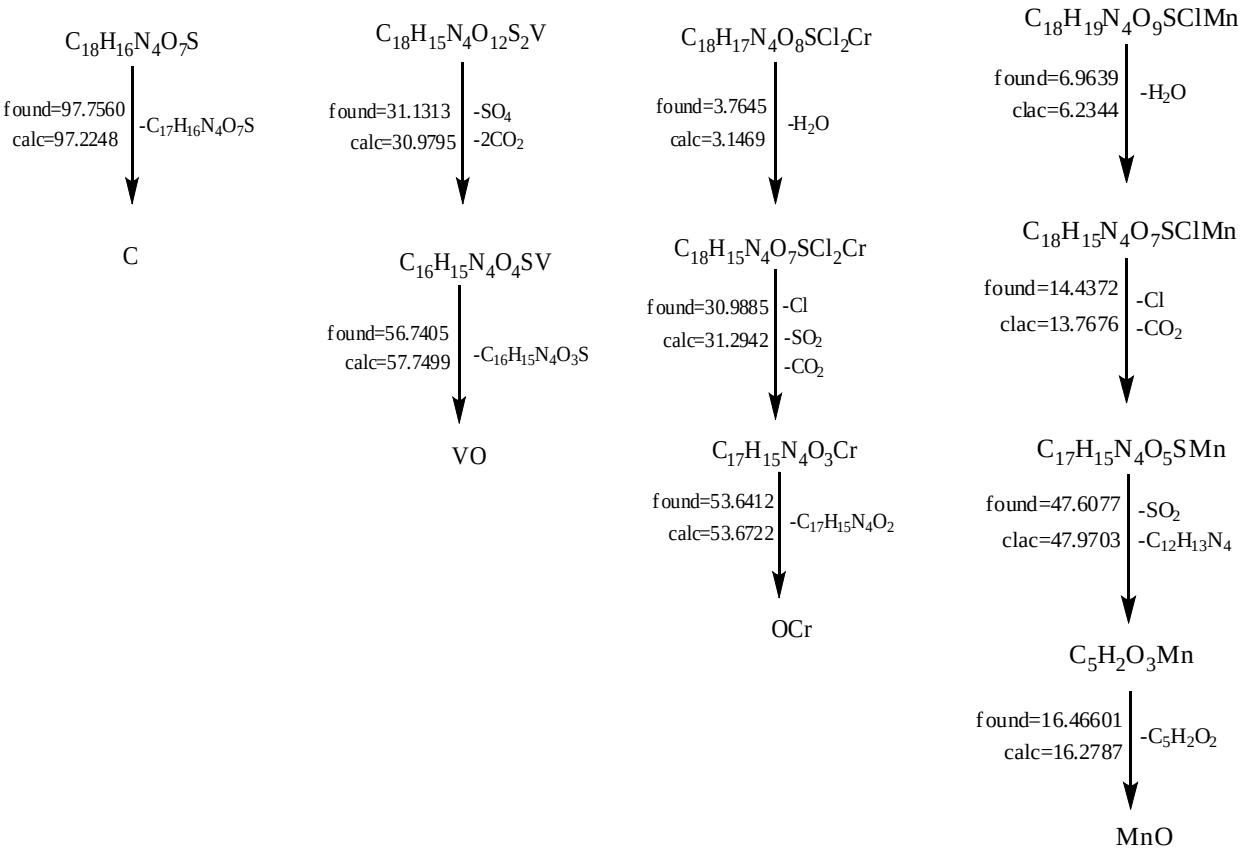

Scheme 7. Tentative decomposition reaction of ligand and metal complexes

Table 5. TGA data of the ligand H_3Landsome complexes

Complexes	Step	T_i/°C	T_f/°C	T_{DTG}max	Weight mass loss%		Reaction
					Calc	**Found**	
Ligand	1	111.021	597.747	347.362	97.2248	97.7560	$-C_{17}H_{16}N_4O_7S$ C
Calculated:97.2248%final=2.7752%;Estimated97.7560%final=2.244%							
V-complex	1	280.102	423.313	317.731	30.9795	31.1313	$-SO_4$, $-2CO_2$
	2	421.678	592.517	498.321	57.7499	56.7405	$-C_{16}H_{15}N_4O_3S$ VO
	Calculated:88.7294% final =11.2706%;Estimated 87.8718% final =12.1282%						
Cr-complex	1	38.200	121.288	80.351	3.1469	3.7645	$-H_2O$
	2	118.998	309.688	251.511	31.2942	30.9885	$-Cl$, $-SO_2$, $-CO_2$
	3	309.799	588.931	419.121	53.6722	53.6412	$-C_{17}H_{15}N_4O_2$ OCr
	Calculated:88.1133% final =11.8867%;Estimated 88.3942% final =11.6058%						
Mn-complex	1	52.111	168.471	109.611	6.2344	6.9639	$-2H_2O$
	2	170.001	242.1	203.721	13.7676	14.4372	$-Cl$, $-CO_2$
	3	247.986	389.359	309.115	47.9703	47.6077	$-SO_2$, $-C_{12}H_{13}N_4$
	4	390.031	597.709	414.413	16.2787	16.4660	$-C_5H_2O_2$ MnO
	Calculated:84.251% final =15.749%;Estimated 85.4748% final =14.5252%						

2024, 21(5): 1512-1535
https://dx.doi.org/10.21123/bsj.2023.8365
P-ISSN: 2078-8665 - E-ISSN: 2411-7986
Baghdad Science Journal

Table 6. Thermal decomposition DSC of Ligand and somecomplexes

Compound	T_i/°C	T_f/°C	Maximum temperature point °C	ΔH J/g	ΔS J	ΔG J	Type
L_3H	387.65	395.13	392.40	-13.49	-1.804	694.399	**endothermic**
$VO(H_2L)(SO_4)$] [	39.23	104.90	66.29	-28.23	-0.430	0.2747	**endothermic**
	209.23	236.59	226.78	-29.09	-1.063	211.977	**endothermic**
	256.98	266.41	266.40	-4.44	-0.471	121.034	**endothermic**
$Cr(H_2L)(H_2O)Cl_2$][	70.38	119.40	99.62	-119.11	-2.430	122.967	**endothermic**
	127.48	188.10	157.80	-227.66	-3.755	364.879	**endothermic**
	204.97	227.99	215.11	-9.22	-0.401	77.039	**endothermic**
	230.45	286.67	251.01	-50.94	-0.906	176.475	**endothermic**
$Mn(H_2L)(H_2O)_2Cl$] [	70.38	119.40	99.62	-119.11	-2.430	122.967	**endothermic**
	127.48	188.10	157.80	-227.66	-3.755	364.879	**endothermic**
	204.97	227.99	215.11	-9.22	-0.401	77.039	endothermic
	230.45	286.67	251.01	-50.94	-0.906	176.475	endothermic

Investigation of Antioxidant Activity

The assay is used to determine how well antioxidants can scavenge it. Antioxidants provide a hydrogen atom to1-(2,4,6-Trihydroxy-phenyl)-ethanone, which reduces the single electrons from nitrogen atoms in DPPH . When the DPPH radical solution is combined with the antioxidant, the color of the corresponding hydrazine changes from violet to yellow, which is characterized by an absorption band in an ethanol solution centered at approximately (517 nm). electron delocalization also produces dark purple[29]. The interaction of $[VO(H_2L)(SO_4)]$, $[Cr(H_2L)(H_2O)Cl_2]$,$[Mn(H_2L)(H_2O)_2Cl]$ and$[Cu(H_2L)(H_2O)_2Cl]$ complexes with DPPH radicals and subsequent hydrogen donation to scavenge the radicals are displayed in Table 7.Effective DPPH radical scavenging is indicated by a lower IC_{50} value. In the DPPH assay, the practically Cr-complex has more antioxidant activity than the metal complexes[30,31].

Table 7. Antioxidant activity of Azo dye and its complexes

Compounds	Mean	Standard deviation	Coefficient of variation%	Correlation coefficient	IC_{50}(M)
GA	93.5600	2.0846	2.2281	0.9993	6.1135
H_3 L	85.7600	3.0663	3.3521	0.9938	4.6630
$Mn(H_2L)(H_2O)_2Cl$][	68.8316	5.7753	4.1123	0.9977	2.6521
$[VO(H_2L)(SO_4)]$	68.2735	3.6742	13.8665	0.9978	2.1663
]$Cr(H_2L)(H_2O)Cl_2$[	71.2276	4.7796	13.8221	0.9993	2.1350
$Cu(H_2L)(H_2O)_2Cl$][	80.3162	2.5007	3.7986	0.9961	2.6651

Conclusion

In summary, we successfully synthesized a new Azo ligand derivatives of sulfamethoxazole by simple substitution reactionfrom with 1-(2,4,6-Trihydroxy-phenyl)-ethanone.Then ligand and metal complexes were characterized by various analytical techniques, like elemental microanalysis, metal – chloride containing, electrical conductivity measurement, magnetic susceptibility,^{1}H and ^{13}CNMR, FT-

2024, 21(5): 1512-1535
https://dx.doi.org/10.21123/bsj.2023.8365
P-ISSN: 2078-8665 - E-ISSN: 2411-7986
Baghdad Science Journal

IR,\UV-Vis , mass spectra, and thermal analysis (TGA and DSC) curves .The DCS curve was used to calculate the thermodynamic parameters ΔH, ΔS, , and Δ G. The yield of the synthesized compounds was found to be in the range from 60-80%. The molar conductivity results showed that none of the produced complexes are electrolytes, and the atomic N ,O and O tridentate coordination sites in the ligand were identified by comparing their IR spectra to those of the metal complexes. The M:L ratio in every compound was [1:1]. According to the results, octahedral geometry suggest of ;(Cr^{3+}, Mn^{2+} and Cu^{2+}), V^{4+}complex square pyramidal .Antioxidant activity of the synthetic compounds were evaluated against the DPPH radical (1.1-diphenyl-2-picrylhydrazyl), and the results were contrasted with those of gallic acid, a widely used natural antioxidant. Results show how efficient metal complexes was at scavenging free radicals.

Acknowledgment

Authors would like to thank everyone that contributed to the success of this review article Department of Chemistry, College of Science for women, Baghdad University, Ministry of Higher Education & Scientific Research & Science and Technology, Directorate of Environment & Water.

Authors' Declaration

- Conflicts of Interest: None.
- We hereby confirm that all the Figures and Tables in the manuscript are ours. Furthermore, any Figures and images, that are not ours, have been included with the necessary permission for re-publication, which is attached to the manuscript.
- Ethical Clearance: The project was approved by the local ethical committee in University of Baghdad.

Authors' Contribution Statement

This work carried out in collaboration between all authors. A. A. S. did the tests and analysis the data with revision. A. M. A. prepared the samples, wrote, and edited the manuscript with revision.

References

1. Ibraheem IH, Mubder NS, Abdullah MM, Al-Neshmi H. Synthesis, characterization and bioactivity Study from azo –ligand derived frommethyl-2-amino benzoatewith some metal ions. Baghdad Sci J. 2023; 20(1): 114-120. https://doi.org/10.21123/bsj.2022.6584
2. Al-Hamdani AAS, Al Zoubi W. New metal complexes of N3 tridentate ligand: Synthesis, spectral studies and biological activity. Spectrochim Acta- A: Mol Biomol Spectrosc. 2015; 137: 75-89. https://doi.org/10.21123/bsj.2022.7289
3. Al Zoubi, W, Al-Hamdani AAS, Ahmed SD, Ko YG. Synthesis, characterization, and biological activity of Schiff bases metal complexes. J Phys Org Chem. 2018; 31(2): e3752. https://doi.org/10.1002/poc.3752
4. Nagasundaram N, Govindhan C, Sumitha S, Sedhu N, Raguvaran K, et al. Synthesis, characterization and biological evaluation of novel azo fused 2, 3-dihydro-1H-perimidine derivatives: In vitro antibacterial, antibiofilm, anti-quorum sensing, DFT, in silico ADME and Molecular docking studies. J Mol Struct. 2022; 1248: 131437.https://doi.org/10.1016/j.molstruc.2021.131437
5. Hamad SF, Ibraheem TK. Synthesis, Characterize and Antibacterial Evaluate of Some Novel Compounds Containing 1, 3, 4-thiadiazole. J Pharm Negat. 2022; (13)3 1119-1122.https://doi.org/10.47750/pnr.2022.13.S03.176
6. Al Zoubi W, Al-Hamdani AAS, Widiantara IP, Hamoodah RG, Ko YG . Theoretical studies and antibacterial activity for Schiff base complexes. J Phys Org Chem. 2017; 30 (12): e3707. https://doi.org/10.1002/poc.3707
7. Turan N, Buldurun K. Synthesis, characterization and antioxidant activity of Schiff base and its metal complexes with Fe (II), Mn (II), Zn (II), and Ru (II) ions: Catalytic activity of ruthenium (II) complex. Eur

J Chem.2018; 9(1): 22-29. https://doi.org/10.5155/eurjchem.9.1.22-29.1671
8. Mohammed H. Synthesis, Identification, and Biological Study for Some Complexes of Azo Dye Having Theophylline. Sci world j. 2021 Jul 22; 2021. https://doi.org/10.1155/2021/9943763
9. Ispir E, Ikiz M, Inan A, Sünbül AB, Tayhan SE, Bilgin S, et al. Synthesis, structural characterization, electrochemical, photoluminescence, antiproliferative and antioxidant properties of Co (II), Cu (II) and Zn (II) complexes bearing the azo-azomethine ligands. J Mol Struct. 2019 Apr 15; 1182: 63-71. https://doi.org/10.1016/j.molstruc.2019.01.029
10. Al Zoubi W, Al-Hamdani AAS, Ahmed SD, Ko YG . A new azo-Schiff base: Synthesis, characterization, biological activity and theoretical studies of its complexes. Appl Organometal Chem. 2017; e3895. https://doi.org/10.1002/aoc.3895
11. Lashanizadegan M, Ashari HA, Sarkheil M, Anafcheh M, Jahangiry S. New Cu (II), Co (II) and Ni (II) azo-Schiff base complexes: Synthesis, characterization, catalytic oxidation of alkenes and DFT study. Polyhedron. 2021 May 15; 200: 115148. https://doi.org/10.1016/j.poly.2021.115148
12. Kyei SK, Akaranta O, Darko G. Synthesis, characterization and antimicrobial activity of peanut skin extract-azo-compounds. Sci Afr. 2020 Jul 1; 8: e00406. https://doi.org/10.1016/j.sciaf.2020.e00406
13. Mahdy AR, Ali OA, Serag WM, Fayad E, Elshaarawy RF, Gad EM. Synthesis, characterization, and biological activity of Co (II) and Zn (II) complexes of imidazoles-based azo-functionalized Schiff bases. J Mol Struct. 2022 Jul 5; 1259: 132726. https://doi.org/10.1016/j.molstruc.2022.132726
14. Kyhoiesh HA, Al-Adilee KJ. Synthesis, spectral characterization, antimicrobial evaluation studies and cytotoxic activity of some transition metal complexes with tridentate (N, N, O) donor azo dye ligand. Results Phys. 2021 Jan 1; 3: 100245. https://doi.org/10.1016/j.rechem.2021.100245
15. Mandour HS, Abouel-Enein SA, Morsi RM, Khorshed LA. Azo ligand as new corrosion inhibitor for copper metal: Spectral, thermal studies and electrical conductivity of its novel transition metal complexes. J Mol Struct. 2021 Feb 5; 1225: 129159. https://doi.org/10.1016/j.molstruc.2020.129159
16. Minnelli C, Laudadio E, Galeazzi R, Rusciano D, Armeni T, Stipa P, Mobbili G. Synthesis, characterization and antioxidant properties of a new lipophilic derivative of edaravone. Antioxidants. 2019; 8(8): 258. https://doi.org/10.3390/antiox8080258
17. Hamza IS, Mahmmoud WA, Al-Hamdani AA, Ahmed SD, Allaf AW, Al Zoubi W. Synthesis, characterization, and bioactivity of several metal complexes of(4-Amino-N-(5-methyl-isaxazol-3-yl)-benzenesulfonamide) . Inorg. Chem Commun. 2022; 144: 109776. https://doi.org/10.1016/j.inoche.2022.10977
18. Unnisa A, Abouzied AS, Baratam A, Lakshmi KC, Hussain T, Kunduru RD, et al. Design, synthesis, characterization, computational study and in-vitro antioxidant and anti-inflammatory activities of few novel 6-aryl substituted pyrimidine azo dyes. Arab J Chem. 2020; 13(12): 8638-8649. https://doi.org/10.1016/j.arabjc.2020.09.050
19. Keshavayya J, Pushpavathi I, Keerthikumar CT, Maliyappa MR, Ravi BN. Synthesis, characterization, computational and biological studies of nitrothiazole incorporated heterocyclic azo dyes. J Struct Chem. 2020; 31(4): 1317-1329.https://doi.org/10.1007/s11224-020-01493-0
20. Moamen SR, Altalhi T , Safyah BB, Ghaferah HA, Kehkashan A. New Cr(III), Mn(II), Fe(III), Co(II), Ni(II), Zn(II), Cd(II),and Hg(II) Gibberellate Complexes: Synthesis, Structure,and Inhibitory Activity Against COVID-19 Protease. Russ J Gen Chem. 2021; 91(5): 890–896. https://doi.org/10.1134/S1070363221050194
21. Reda SM, Al-Hamdani AAS. Mn (II), Fe (III), Co (II) and Rh (III) complexes with azo ligand: Synthesis, characterization, thermal analysis and bioactivity.Baghdad Sci J. 2022; 91(5):890-896. https://doi.org/10.21123/bsj.2022.7289
22. Maliyappa MR, Keshavayya J, Mallikarjuna NM, Krishna PM, Shivakumara N, Sandeep T, et al. Synthesis, characterization, pharmacological and computational studies of 4, 5, 6, 7-tetrahydro-1, 3-benzothiazole incorporated azo dyes. J Mol Struct. 2019; 1179: 630-641.https://doi.org/10.1016/j.molstruc.2018.11.041
23. Al-Daffay RK, Al-Hamdani AA. Synthesis, Characterization, and Thermal Analysis of a New Acidicazo Ligand's Metal Complexes. Baghdad Sci J. 2022; 19(3): 121-33. : http://dx.doi.org/10.21123/bsj.2022.6709
24. Turan N, Buldurun K. Synthesis, characterization and antioxidant activity of Schiff base and its metal complexes with Fe (II), Mn (II), Zn (II), and Ru (II) ions: Catalytic activity of ruthenium (II) complex. Eur J Chem. 2018 Mar 31; 9(1): 22-9. https://doi.org/10.5155/eurjchem.9.1.22-29.1671
25. EL-Gammal OA, Alshater H, El-Boraey HA. Schiff base metal complexes of 4-methyl-1H-indol-3-carbaldehyde derivative as a series of potential antioxidants and antimicrobial: Synthesis, spectroscopic characterization and 3D molecular modeling. J Mol Struct. 2019 Nov 5; 1195: 220-30. https://doi.org/10.1016/j.molstruc.2019.05.101

2024, 21(5): 1512-1535
https://dx.doi.org/10.21123/bsj.2023.8365
P-ISSN: 2078-8665 - E-ISSN: 2411-7986
Baghdad Science Journal

26. Al Zoubi W, Al-Hamdani AAS, Susan DA, Hassan MB, Al-Luhaibi RSA, Dib A, Young GK. Synthesis, characterization, and antioxidant activities of imine compounds. J Phys Org Chem. 2019; 32(3): e3916. https://doi.org/10.1002/poc.3916
27. Olesya S, Alexander P. Antimicrobial activity of mono-and polynuclear platinum and palladium complexes. Foods Raw Mater. 2020; 8(2): 298-311.http://doi.org/10.21603/2308-4057-2020-2-298-311
28. Rezaei-Seresht E, Salimi A, Mahdavi B. Synthesis, antioxidant and antibacterial activity of azo dye-stilbene hybrid compounds. Pigm Resin Tchnol. 2019; 48(1): 84-88. https://doi.org/10.1108/PRT-01-2018-0005
29. Kareem MJ, Al-Hamdani AAS, Ko YG, Al Zoubi, W, Mohammed Saad G. Synthesis, characterization, and determination antioxidant activities for new Schiff base complexes derived from 2-(1H-indol-3-yl)-ethylamine and metal ion complexes. J Mol Struct. 2021; 1231: 129669. https://doi.org/10.1016/j.molstruc.2020.129669
30. Turan N, Buldurun K, Adiguzel R, Aras A, Turkan F, et al. Investigation of spectroscopic, thermal, and biological properties of Fe(II), Co(II), Zn(II), and Ru(II) complexes derived from azo dye ligand. J Mol Struct. 2021 Nov 31; 1244: 130989. https://doi.org/10.1016/j.molstruc.2021.130989
31. Al-Hamdani AAS, Al-Alwany TAM, Mseer MA, Fadhel AM, Al-Khafaji YF. Synthesis, Characterization, Spectroscopic, Thermal and Biological Studies for New Complexes with N1, N2-bis (3-hydroxyphenyl) Oxalamide. EgyptJ. of Chem. 2023 66(4): 223-235. 10.21608/EJCHEM.2022.144403.6297

تحضير ، تشخيص دراسة التحلل الحراري فعالية مضادات الاكسدة لمعقدات العناصر الانتقالية مع ليكاند صبغة الازو

أمنه مهدي عبدالله، عباس علي صالح الحمداني

قسم الكيمياء، كلية العلوم للبنات، جامعة بغداد، بغداد، العراق.

الخلاصة

تم إجراء تفاعل ديازوتيزيشن بين 1- (6,4,2-ثلاثي هيدروكسي-فينيل) -إيثانون وأملاح ديازونيوم مما أدى إلى تكوين ليكاند 4- (3-أسيتيل -2،4،6-ثلاثي هيدروكسي-فينيل ازو) -5) -N-ميثيل-إيزوكسازول-3-يل) -بنزين سلفوناميد ، وهذا بدوره يتفاعل مع أيونات المعادن التالية (V^{4+}، Cr^{3+}، Mn^{2+} و Cu^{2+}) مكونة معقدات مستقرة ثمانية السطوح لكل من الكروم والمنغنيز والنحاس و هرمي مربع القاعدة للفناديوم الرباعي .تم اكتشاف إنشاء مثل هذه المعقدات من خلال استخدام الوسائل الطيفية التي تنطوي على الأشعة فوق البنفسجية التي أثبتت الأشكال الهندسية التي تم الحصول عليها ، وأثبت IR تكوين مجموعة الآزو والتنسيق مع أيون المعدن من خلالها. أثبتت دراسات الانحلال الحراري (TGA & DSC) تنسيق بقايا الماء مع أيونات المعادن داخل مجال التناسق وكذلك ذرات الكلور. علاوة على ذلك ، التحليل الجزئي للعنصر و AAS الذي أعطى النتيجة المقابلة مع نتيجة العد النظري. (^{1}H &^{13}C-NMR) والكميات المغناطيسية يمكن أن تشير أيضًا إلى تكوين ليكاند H_3L وحدوث التنسيق. تم حساب الثوابت الديناميكية الحرارية (ΔH, ΔS, ΔG). سيتم استخدام طريقة الكسح الجذري DPPH لتقييم الأنشطة المضادة للأكسدة للمركبات التي أظهرت قدرتها المضادة للأكسدة على اخماد الجذور الحرة.

الكلمات المفتاحية: مضادات الاكسدة, صبغة ازو, مطيافية الكتلة, 1-(6,4,2 ثلاثي هيدروكسي- فينيل)- ايثانون, التحليل الحراري.